Solar RRL

High-Throughput Characterization of Perovskite Solar Cells for Rapid Combinatorial Screening

--Manuscript Draft--

Manuscript Number:	solr.202000097R1
Article Type:	Full Paper
Corresponding Author:	Udo Bach Monash University Clayton, AUSTRALIA
Corresponding Author E-Mail:	udo.bach@monash.edu
Order of Authors:	Maciej Adam Surmiak, PhD Candidate
	Tian Zhang, PhD
	Jianfeng Lu, PhD
	Kevin James Rietwyk, PhD
	Sonia Ruiz Raga, PhD
	David Patrick McMeekin, PhD
	Udo Bach, Professor (Full)
Keywords:	high-throughput perovskite solar cell characterization; 16-channel potentiostat real-time measurements; MPPT; perovskite solar cell performance and stability; materials discovery
Section/Category:	
Abstract:	In order to discover the ideal perovskite material for solar cell application, a large parameter space (composition, surrounding condition, fabrication technique etc.) must first be explored. Hence, screening this parameter space using a rapid combinatorial screening approach could drastically speed-up the rate of discovery. During the last decade, these discoveries and optimization processes of perovskite materials have been achieved using simple lab-scale deposition techniques and characterization methods, resulting in a substantial time-consuming process, slowing the rate of progress in field of photovoltaics. Thus, the benefits of developing fully-automated, high-throughput characterization techniques become apparent. In this paper, we detail a high-throughput solar cell testing system that enables parallel, real-time and comprehensive measurements, allowing for 16 solar cells to be characterized simultaneously. We show the importance of measurement reproducibility, condition verification and structured data post-processing.
Author Comments:	
Additional Information:	
Question	**Response**

Please submit a plain text version of your cover letter here.	Article: High-Throughput Characterization of Perovskite Solar Cells for Rapid Combinatorial Screening Authors: Maciej Adam Surmiak, Tian Zhang, Jianfeng Lu, Kevin James Rietwyk, Sonia Ruiz Raga, David Patrick McMeekin, Udo Bach Dear Prof Hildebrandt, We are pleased to submit the attached manuscript to you for consideration for publication in Rapid Research Letters. In this work, we addressed ongoing discussion about the correct protocol for Perovskite Solar Cell characterization. We designed and built a high-throughput instrument which allows comprehensive, reproducible and accurate measurement of 16 solar cells in parallel (simultaneously without any sequential delay). Our system employs a 4-wire sense technique which we show, it identifies and reduces parasitic series resistance which is not addressed across all the literature. It also employs direct measured device temperature and humidity control, crucial for accurate analysis. Once samples are loaded in their customized jig, the electrical analysis and data post-processing is launched. The fully automatized measurement minimizes time spent by a factor of 10, reduces human-error and saves researcher-time whilst employing precision and novel characterization protocols which can be crafted to specific type of perovskite before the measurement. We believe that adjustable protocol for high-throughput study should contribute to on-going discussion about perfect choice of pre-sets and characterization reports. We believe our work meets the high standards of Rapid Research Letters Solar. This work represents significant progress in high-throughput characterisation of solar cells and is suitable for rapid optimization of fabrication procedures and material discovery. As such, we are certain that it will be among the most influential in its field and of great interests to a broad readership. The work described has not been submitted elsewhere for publication, in whole or in part. The manuscript was reviewed and approved for submission to your journal by all of the authors listed. Thank you for your consideration. Sincerely, Prof. Udo Bach
Do you or any of your co-authors have a conflict of interest to declare?	No. The authors declare no conflict of interest.
Response to Reviewers:	

ORIGINAL ARTICLE

Journal Section

High-Throughput Characterization of Perovskite Solar Cells for Rapid Combinatorial Screening

Maciej Adam Surmiak[1*] | Tian Zhang[2†] | Jianfeng Lu[2†] | Kevin James Rietwyk[2†] | Sonia Ruiz Raga[2†] | David P McMeekin[2†] | Udo Bach[2]

[1]Department of Chemical Engineering, Monash University, Victoria 3800, Australia

[2]ARC Centre of Excellence for Exciton Science, Monash University, Victoria 3800, Australia

Correspondence
Professor Udo Bach, Chemical Engineering, Monash University, Clayton, Victoria, 3800, Australia
Email: udo.bach@monash.edu

Present address
[†]Chemical Engineering, Monash University, Clayton, Victoria, 3168, Australia

Funding information
The authors are grateful for the financial support of this work by the Australian Centre for Advanced Photovoltaics (ACAP), the Australian Renewable Energy Agency and the ARC Centres of Excellence in Exciton Science (ACEX; CE170100026)

In order to discover the ideal perovskite material for solar cell application, a large parameter space (composition, surrounding condition, fabrication technique etc.) must first be explored. Hence, screening this parameter space using a rapid combinatorial screening approach could drastically speed-up the rate of discovery. During the last decade, these discoveries and optimization processes of perovskite materials have been achieved using simple lab-scale deposition techniques and characterization methods, resulting in a substantial time-consuming process, slowing the rate of progress in field of photovoltaics. Thus, the benefits of developing fully-automated, high-throughput characterization techniques become apparent. In this paper, we detail a high-throughput solar cell testing system that enables parallel, real-time and comprehensive measurements, allowing for 16 solar cells to be characterized simultaneously. We show the importance of measurement reproducibility, condition verification and structured data post-processing.

KEYWORDS
Perovskite Solar Cell, Characterization, High-throughput

Abbreviations: ARC, Australian Research Council; ACEX, Australian Centre of Excellence in Exciton Science

[*]Equally contributing authors.

1 | INTRODUCTION

In the past decade, there has been a drastic upheaval in the research of photovoltaics with the introduction of solution-processed solar cells, particularly inorganic-organic hybrid lead halide perovskite materials. Perovskite materials have a general ABX_3 chemical formula, where A is a cation, B a divalent metal ion, and X a halide. Moreover, by adjusting the chemical composition of the A-site cation, commonly, (methylammonium, and formamidinium, or caesium), the B-site metal cation (lead or tin) or the X-site anions (iodide, bromide, chloride) we can fine-tune the optoelectronic properties of this novel semiconductor. Perovskite solar cells (PSCs) have achieved significant power conversion efficiencies that are currently competing with commercially available solar cells.1 Their performance continuously improved over the past decade, reaching a certified power conversion efficiency (PCE) of 25.2%1, rivalling the all-time champion silicon solar cells (SCs) with record efficiencies of 26.1%1. However, the characterization of PSC is non-trivial due to their ionic movement within the material, resulting in a range of transient behaviors when attempting to measure their performance.2 Due to this ionic movement within the film when a voltage bias is applied, a hysteric behavior is observed during the measurement of the current-voltage (*J-V*)3-5 curve. To eliminate the effect of ionic motion when determining the true performance of the device, a maximum power point tracking (MPPT) technique is preferred over a *J-V* scan.6 Furthermore, to mitigate the effect of heating caused by 1 Sun illumination, which can reach 35-40°C, the device is held at 25°C using a nitrogen gas flow7-8, when illuminated with a spectral irradiance of AM 1.5G and a 1000 W/m^2 power density using a lamp (xenon, quartz tungsten halogen, metal halide or light-emitting diode)9-10 and area-defining mask. The ionic behavior of lead halide perovskites causes a hysteric behavior in the *J-V* curve, depending on scan parameters such as: scan direction, speed, settling time and bias voltage range. These devices also demonstrate severe memory-like effects, where the performance is altered by past measurement such as: light soaking, applied voltage bias, storage under specific atmospheres and temperatures. Recently, Zimmermann *et al*., Pellet *et al*. and Rakocevic *et al*. addressed the complex challenges in reliability of the measurements.6, 11-12 Perovskite laboratories around the world have their own ad-hoc *J-V* measurement protocols, thus causing ambiguity when reporting the true performance of the solar.12-16 11 Despite the aforementioned issues, *J-V* scans still remain a key characterization tool amongst the perovskite research community. The most reliable method for measuring a *J-V* curve, is the dynamic *J-V* curve, where the current-density for each voltage point is measured long enough to demonstrate stable current).17 Although this method is highly accurate and only requires a sweep in a single direction, this approach takes longer to perform compared to a conventional *J-V* curve (where, the extracted current is stabilized over a period of time determined by the user. Therefore, the generally agreed best approach to determine the stabilised PCE is to track the evolution of the extracted current at maximum power point voltage over the course of typically 1-10 minutes. Similarly, to obtain a stabilised measurement of the short-circuit current density (J_{SC}), and open-circuit voltage V_{OC}, a time-depend approach can be utilised. Another approach to obtain a stabilized *J-V*, involves repeating the measurement of the *J-V* curve until the curve stabilizes, thus, accounting the impact of "light-soaking". 16, 18-19 However, each method has their own shortcomings, hence, to account for the fluctuation in maximum power point (V_{MPP}) over time, while also minimizing the measurement time, a maximum power point tracking (MPPT) is viable approach as a characterising method. Dunbar *et al*. recently reported an inter-laboratory comparison on the measurement of perovskite solar cells that highlights the variability in measurement protocol across 10 laboratories.15 One of the key findings was that the variability in measured PCE for each laboratory was primarily determined by light and voltage pre-conditioning, electrical measurement protocol and inaccuracies in estimating the cell active area. The manual handling of the devices during the fabrication and characterization and the arbitrary choice of measurement parameters contribute to difficulties when comparing PCE from lab-to-lab. Therefore, in order to bolster research outcomes, it is preferred to automatize and standardize such routine electrical characterizations and develop MPPT algorithms to

accurately report PCE. Only a few commercial solar cell measurements systems are available today, however, they usually do not achieve all three desired requirements for PSC research: (i) customisation of measurement parameters and protocols, (ii) simultaneous measurement of several devices and (iii) a sample holder to precisely overlap the aperture mask with the counter electrodes. Due to lack of versatile commercial instruments crafted specifically for perovskite solar cells, many researchers decide to design their own characterization set-ups, based on programmable source-measure units (NI, Ossila, Keysight or Keithley). Some of the commercial products offer automated computation of key characterization parameters commonly found across solar cell research, however, these parameters are not necessarily tailored towards the specific needs of PSCs, such as light and bias pre-conditioning, or versatility in selecting *J-V* parameters such dwell time or scan speed to mitigate the impact of the hysteretic behavior found in PSC. These measurement instruments were designed to cater to the for solid state solar cell industry, which do not exhibit strong transient behavior when being measured. Here we present a systematic study using a versatile state-of-the-art high-throughput solar cell characterization system, capable of testing up to 16 solar cells simultaneously, while maintain a high level of reproducibility. We demonstrate the advantages of the system in terms of accuracy, speed and reproducibility, with our results captured in less than one tenth of the measurement time compared to conventional approaches. We believe that this system will provide a valuable guidance for researchers, when characterizing PSC with hysteretic behavior and consequently will play an important role in developing future measurement system for the photovoltaics (PV) industry. 42-47

2 | RESULTS AND DISCUSSION

At research-scale, solar cell devices are generally fabricated on individual substrates of area less than 5 cm^2 due to size limitations posed by laboratory equipment, and in order to reduce research costs. The laboratory fabrication process for PSC test cells typically involves the manual cutting of transparent conductive oxides (TCO) substrates by hand tools, which results in poorly controlled substrate shapes and sizes. The manual cutting and patterning require extra care and extensive cleaning and despite efforts of being precise manual cutting causes significant glass size difference (± 1 - 3 mm) making the use of precise jig and masking impossible. In order to address these bottlenecks for high throughput solar cell research, we combine a number of techniques to reduce the manual handling using a jig (positioning device) based fabrication (Supplementary Information, S1). Firstly, we increased the number of solar cells per substrate. The old substrates were diced by hand from 100x100 mm of fluorine-doped tin oxide (FTO, < 14 Ω/sq.) to ± 25 x 25 mm pieces. New ones are commercially ordered as precision-cut, pre-patterned pieces covered with a thin film of fluorine-doped tin oxide (FTO, < 10 Ω/sq.). For that, we have designed a new substrate architecture that can contain four individual solar cells electrically isolated from each other (see Fig. 1A). Custom-made, precision-cut, pre-patterned FTO glass substrate (accuracy ± 0.15 mm) were sourced from Latech Scientific Supply Pte Ltd (Singapore). The glass is cleaned in specially ordered trays which are placed in ultrasonic baths. Cleaned substrates are dried and placed in precisely milled jig. The automated way of spraying TiO_2 therefore allows minimizing discrepancy of layer thickness and quality from batch to batch. The ETL covered substrates are therefore transported to glovebox where spin coating of perovskite precursor solution and HTL is performed. Later on, the substrates are placed in another precisely milled jig in order to evaporate Au electrodes making the alignment and masking procedure completely redundant, ensuring the same position of the electrodes across entire batch of solar cells. We have encompassed in the design that the tolerance build-up between each commercially purchased substrate (up to ± 0.15 mm), position in the measurement pocket (± 0.016 mm) and evaporation plate (± 0.01 mm) can negatively influence results, so therefore we have designed the connection printed circuit board (PCB) accordingly. The pin rows are positioned in

the middle of 2 mm wide contact electrode areas; thus, the connection is always established. We highlighted the fabrication differences in fabrication step in Tab.1.

TABLE 1 Comparison between fabrication steps of new and old design solar cell.

Variables	Alignment required	Old method	New method
Glass cutting	Y	Hand scribe and cut	Precision laser cut (± 0.15 mm)
Pattern etching	Y	Manual	Laser pattern (± 0.001 mm)
Compact TiO_2	Y	Manual	Automated spray inside of jig*
Mesoporous TiO_2	N	Jig not required	Jig not required
Perovskite	N	Jig not required	Jig not required
Spiro-OMeTAD	N	Jig not required	Jig not required
Edge removal	Y	Solvent cleaning	Machine buffing
Gold evaporation	Y	Tape masking	CNC milled jig (± 0.01mm)
Shadow mask	Y	Manually placed	Guided and magnet-clamped

*jig - device used for positioning.

2.1 | Methodology

We designed a custom-made sample holder (Fig. 1D) that allows for the simultaneous measurement of four substrates, containing four solar cells. The holder allows for precise alignment between the aperture mask and the active area, further details on the sample mounting are presented in Fig.1B,C. In addition, the holder has built-in sensors for temperature and relative humidity, as well as a Si photodiode reference cell with KG5 filter. The chamber also has ports and lines for N_2 gas circulation, directed onto the solar cells to reduce the presence of oxygen and moisture, while simultaneously providing an active cooling during the measurement process. All sensors, photodiode and N_2 valves are communicating with the computer through a microcontroller (ATmega 2560), giving full access to the end user. The 16 solar cells are connected to a commercially available, computer controlled, 16-channel potentiostat (Bio-Logic VMP3). The holder provides electrical contact by utilising a magnetic lid to press the solar cells onto the spring loaded pins. The custom-built PCB board is mounted inside of the sample to provide good contact connection between the pin and electrode. We have used a two-fold-redundancy system to always achieve electrical contact connection. The sample holder is mounted on a motorized two-axis (x-y) stage that is connected to the PC through a second microcontroller. The moving stage allows the light intensity to be mapped using the reference Si solar cell, then the solar cells are placed in the region with greatest illumination uniformity; this will be explained in detail in Section 2.3. Moreover, the x-y moving stage could potentially host several sample holders to further increase the throughput of the solar simulator by sequentially measuring batches of 16 devices. The motorized stage is aligned with a commercial solar simulator (Abet Technologies Sun 3000 class AAA). The solar simulator is equipped with a software-operated built-in programmable light shutter wired to one of the microcontrollers. Finally, the system is controlled by a custom-made piece of LabView software; further details on the characteristics of the protocol are provided in Section 2.3; for picture see Supplementary Information, S2.

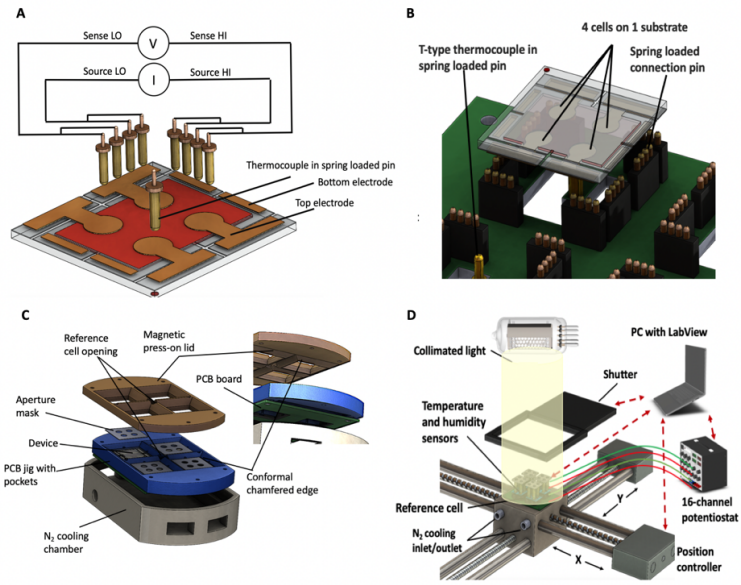

FIGURE 1 Schematic diagram of the high-throughput solar cell characterization system. (a) A schematic showing a custom-designed pre-patterned FTO substrate that is being probed in a 4-wire sense configuration with spring-loaded pins. (b) Close up of a single substrate slot, where each cell is connected with 8 spring loaded pins, and measured with a 4-wire sense technique. (c) Single measurement module consists of positioning jig where the substrates are mounted, the design allows the room for a thin 0.08 mm black dyed stainless-steel apertures masks. The masks are pressed against the solar cells by a magnetic force and the chamfered protrusion guides the magnetic lid in place restricting the movement of the cells and ensuring electrical connection between solar cells and spring-loaded probes. (d) Sample holder consists of a printed circuit-board (PCB) equipped with spring loaded gold pins that provide electrical connection between the 16 solar cells and the potentiostat. The red dashed lines denote communication routes between PC and system parts.

The devices were made in the following way, the substrates are cleaned using Hellmanex® 2% DI water solution, DI water, solvents: acetone, ethanol, isopropanol, respectively and place in an ultrasonic bath for 15 minutes. Onto the FTO a compact layer 10-20 nm of TiO_2 is deposited using spray-pyrolysis. For this, 1 mL of bis(isopropoxide)-bis (acetylacetonate)titanium(IV) dissolved in 19 mL of anhydrous isopropanol at 500°C. Subsequently a mesoporous TiO_2 layer 150-200 nm was spin-coated at 4000 RPM for 20 s with a ramp of 2000 RPM/s using a 30 nm of Dyesol 30 NR-D diluted in ethanol (30 NR-D: ethanol = 1:6, wt.). After that the substrates were dried at 110°C (10 minutes), then they were annealed at 500°C (30 minutes). This was followed by preparation of perovskite films prepared entirely in a N_2 filled glove box including spin coating and annealing and preparation of the precursor solutions. Perovskite precursor solutions were produced by dissolving FAI (1.1 M (M = mole L-1), PbI_2 (1.2 M), MABr (0.22 M), $PbBr_2$ (0.24 M), and CsI (0.07 M) in anhydrous dimethylformamide (DMF):dimethyl sulfoxide (DMSO) (4:1 v/v) to achieve

a composition of $Cs_{0.05}FA_{0.79}MA_{0.16}PbI_{2.49}Br_{0.51}$ with a concentration 1.44 M. The perovskite film was fabricated by spin-coating 80 L of the perovskite precursor solution per substrate using a 2-step program: 1000 RPM for 10 s (1000RPM/s ramp), followed by 6000RPM for 20 s at (6000RPM/s ramp). Then 200 L of chlorobenzene was poured onto the spinning substrate 5 s prior to the end of the second step. The samples were annealed in the dark at 100°C (1 hour) and then allowed to cool to 25°C. After cooling, 80 L of a chlorobenzene solution containing spiro-OMeTAD (60 mM), 4-tert-butylpyridine (tBP; 198 mM), bis(trifluoromethanesulfonyl) imide (LiTFSI; 30 mM), with (1.8 mM) cobalt complex FK269(III), was spin-coated at 3000 RPM for 30 s (3000 RPM/s ramp). A gold (Au) counter-electrode (80 nm) was then deposited on the HTM layer by thermal evaporation. To minimize the possibility of having unconnected cell we used a row of 4 soft spring-loaded pins, having more pins also minimizes damaging of the 80 nm thick metal electrode. This allowed to minimize mechanical damage to the electrodes. Every solar cell is connected with 8 pins in total. To address the issue of the unwanted contact resistance and cable resistance, we implemented a 4-wire sense connection (see Fig.1A). The testing current is applied to the outer pair of contacts and the voltage is measured with the inner pair, for each electrode. The measurement performed at high impedance, thus eliminating the current and voltage drop caused by the contact resistance and the resistance of the external measuring circuit.15 To ensure precision, we designed a thin (0.08 mm) stainless steel opaque aperture mask with a laser-cut opening (0.16 cm^2 ± 0.001 cm^2), to create a precise and well-defined aperture to illuminate the device under test (DUT). Precise of fabrication of this aperture mask is essential to accurately control the active area of the illuminated device and to determine the PCE. We performed a study to establish the optimal ratio between the gold electrode and illumination mask diameter (see Fig. 2). Similarly, it has been demonstrated in Dye-sensitized Solar Cells (DSC) by Ito *et al*. (2006) that the aperture mask size in comparison to the electrode area impacted performance.25 By masking the cells we mitigate any artificial V_{OC} gains.26

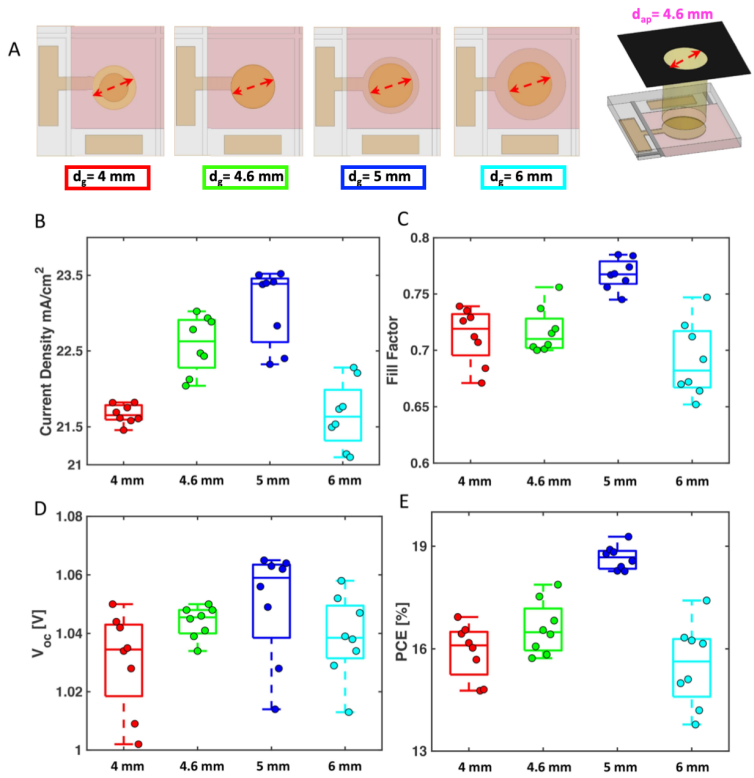

FIGURE 2 Influence of gold electrode diameter (d_g) on PSC performance. A) Schematic illustration of the measurement conditions. PSCs with 4 different gold electrode diameters, ranging from 4 to 6 mm were fabricated and their photovoltaic performance tested, using a shadow mask with a fixed aperture (d_{ap}) of 4.6 mm (red double arrow). The mask was placed on top of the PSC to define the illumination area. B)-D): Photovoltaic performance (short circuit current density (B), fill factor (C), open circuit voltage (D) and power conversion efficiency (E))as a function of gold electrode diameter. Every batch is composed of 8 solar cells. Short circuit current densities are calculated as the ratio of short circuit photocurrent and the illumination area (πr_{ap}^2).

A key concern with performing simultaneous characterization of multiple cells on a single substrate is the possibility of a crosstalk, i.e. current flow between adjacent cells, thus impacting the *J-V* measurement. Despite the wide 0.5 mm pseudo-moat separating the four cells of the patterned FTO glass substrate, lateral current leakage may potentially occur through the perovskite layer, or the HTM or ETL. We investigated case where one, two, three and four cells are illuminated and one is completely covered (see Fig.3). The purpose was to exclude a cross-talk parasite effect from 1,2 and 3 devices measured simultaneously. By scanning the J-V across 4 cells with three exposed cells and one completely masked. We have also measured current below 0.01 mA/cm². The short-circuit current density of illuminated cells exceeds 20 mA/cm², while shaded cells exhibit no significant photocurrent, indicating that the design of the patterned substrate connections and masking is highly effective to impede the crosstalk, for the materials employed (i.e.$Cs_{0.05}FA_{0.79}MA_{0.16}PbI_{2.49}Br_{0.51}$, TiO_2, and Li-TFSI-doped spiro-OMeTAD).18, 27

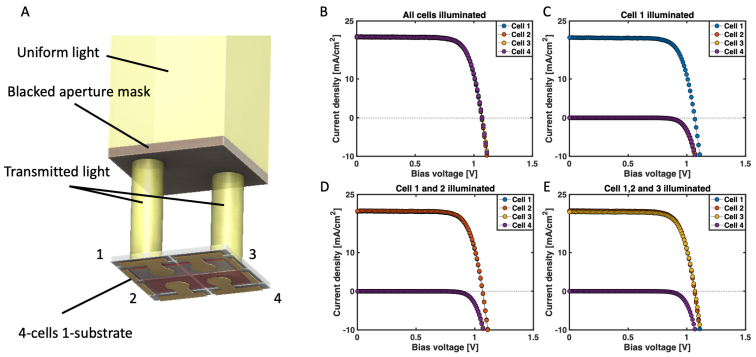

FIGURE 3 Evaluation of cross-talk between solar cells co-located on the same substrate. A) Schematic of a substrate with four solar cells during current-voltage measurement. The mask is precisely clamped on top of the measured device. B)-D) Current density - voltage characteristics recorded in parallel for all 4 devices with specific cells illuminated with simulated AM1.5 (100mW/cm^2) sunlight through a d_{ap} = 4.6 mm aperture mask as indicated.

2.2 | Illumination and external conditions

For research purposes, solar cells are measured under a standardized light source; this enables reproducibility and comparison among laboratories around the world. A xenon lamp light sources emits an electromagnetic spectrum that closely matches the sunlight that reaches the Earth surface after correction of spectral and intensity loss caused by atmospheric gases. This is achieved by using a filter that corrects the xenon spectra to AM1.5, corresponding to a zenith angle of 48.2° and adjusting the lamp power (100 mW/cm^2). 28 The highest class of solar simulators is AAA, which fulfils strict requirements including a uniformity of irradiance of less than 2% across the region of interest and exhibit spectral agreement with the AM1.5G solar spectral of within ± 25% at any wavelength. The overall irradiance of the solar simulator is typically determined using a certified reference Si solar cell with a KG filter.24, 29-30 However, as the lamp ages, the illumination intensity may fluctuate, thus regular monitoring of the actual irradiation power density with a calibrated reference cell prior to the measurements is advisable. To this end, we have integrated a reference Si solar cell in the x-y motorised stage and a simple LabView® code, allowing the user to routinely map the illumination from the solar simulator and confirm that a 1 ± 0.02 Sun equivalent is maintained across the region of interest. An example is given in Figure 4. The program identifies the x-y coordinates for the area with less deviation to 1 Sun intensity and automatically places the sample holder under that region to proceed with the electrical measurements. This ensures a comparable light intensity for each of the cells measured simultaneously and provides a useful tool for gauging the aging on the xenon lamp.

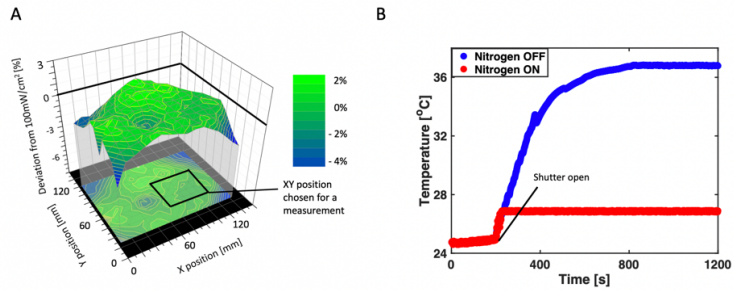

FIGURE 4 A) Spatial map of the relative solar intensity under the solar simulator. The ideal region for analysis is where the deviation is closest to 0%. B) Temperature of the substrate with and without N_2 cooling. The temperature fluctuations in presence of N_2 gas flow are smaller and the temperature after opining the shutter remains at lower level than without active cooling.

2.3 | Electrical characterization of PSCs

As we have mentioned, due to the hysteric behaviour of PSCs, we have designed the software to allow the end-user to vary each electrical parameter according to standard measurements, such as: scan direction, initial voltage, end voltage, scan rate or scan speed, the number of sampling points or voltage step and dwell time or settlement time. In addition, the following pre-conditioning options are available: set an applied voltage and/or open the shutter and light-soak for a certain time a priori to measurement, open the gas valve to purge the chamber and cool the sample before measurement. The user can test stability of the cell by setting the bias voltage and measure the extracted current of up to 16 cells simultaneously. Finally, our software can automatically track the MPP (up to 16 devices in real-time parallel algorithm) where the MPP is sampled up to every 12 seconds to ±10 mV around the previous value and obtains the real-time MPP. The widely discussed in the literature differences between MPPT evolution amongst various perovskite and carrier transport layer (CTL) prompted us to address findings as such.11-12, 14 The most importantly we do not define one and only good characterization method, but rather we implemented possibility to choose between different parameters (voltage step size, voltage dwell time, stabilized transient current test). The users can pick their own parameter set, which is specific for the measured solar cell composition. Furthermore, the user defines the light soaking and gas exposure time,31 and aperture mask area.32 (protocol details and automatically produced statistics can be found in Supplementary Information, S3 and S4) The temperature of substrates was measured before the measurement at 24.2 °C with the relative humidity of the room measured to be RH = 41.2 %. Prior to performing measurements, the solar cells are exposed to N_2 flow for 30 s. We have mapped (system has option of systematic mapping to establish the lamp aging intensity decay) the illumination area to ensure that we are under simulated air mass (AM) 1.5 solar illumination of 100 mW/cm^2. We have chosen 5 s of light soaking prior to scanning at 0 V bias voltage. The voltage was swept from -0.2 to 1.2 V at a scan speed of 80 mV/s with voltage-steps of 10 mV. An *J-V* sweep was initially performed in the dark (solar simulator shutter closed) followed by forward and reverse scans under illumination. We have performed 4 separate tests of 16 solar cells using automated and manual methods. The obtained data from these measurements is presented on Fig. 5. To demonstrate the effectiveness of the solar cell characterization system in terms of accuracy and speed, we proceed to compare the experimental results of 4 batches of 16 solar cell (batches are denoted with A, B, C, D on Fig.5), totalling 64 measurements using first the 16-channel system and comparing it to a single cell manual clipping measurement where each cell is simply connected with alligator clip. An experienced researcher requires an average of 2 min for aligning and fixing the illumination mask,

clipping the two electrodes and placing it perpendicularly to the illumination beam of the solar simulator. Afterwards, an average of 2 min is consumed for sample data entry and running the *J-V* measurement. This protocol, repeated 16 times, resulted in a total of 60 min for the manual measurements, whereas for the automated measurement the devices were mounted simultaneously measured within 5 min. This full automation designed to increase characterization speed is motivated by combinatorial screening in order to discover and optimize novel perovskite compounds. Saliba *et al.* presented a positively trending correlation between the number of fabricated and characterized cells and their overall performance.33 On average, a research laboratory can produce daily 10-20 cells per person hence by having an automatized measurement, we can not only speed up the characterization, but as well make sure that the fabricated devices are treated equally and none of them needs to wait in queue in order to be characterized. As aforementioned, the negative impact of external conditions can significantly degrade the cells and potentially derail the research of a prospecting composition/material/architecture of PSC. The test cells and hence the photocurrents are typically small. In our case I_{SC} < 4 mA. It is often perceived that the 4-wire sense (4WS) is not required, when measuring such small currents. However, the statistical data provides clear evidence that commonly overlooked parasite resistances influenced measurements. All data points come to sit underneath the diagonal indicative of a systematic underestimation of PV performance parameters when using 2-wire sense (2WS). In average this resulted in an underestimation of the PCE of 1-2%. This highlights the importance of using 4WS when measuring PSC test cells using contact pins. In case of 2WS the resistances of test leads and contacts are unknown, hence the voltage drop caused by the sum of all resistances contributed by wires and contact affects the measurement.34 According to literature 41,48 the *FF* is governed by following equations:

$$FF_0 = \frac{V - ln(V + 0.72)}{V + 1} \quad (1)$$

$$FF = FF_0[1 - R_S]x[1 - \frac{1}{R_{SH}}] \quad (2)$$

where V is a normalized V_{OC} corresponding to q/nk_BT (q - elementary charge; n - ideality factor; k_B - Boltzmann constant; T absolute temperature). FF is strongly related to series resistance (R_S) and less to shunt resistance (R_{SH}). The differences in mechanisms between 2WS and 4WS, including bypassing of the test lead and contact resistance is presented in Supplementary Information, S5.

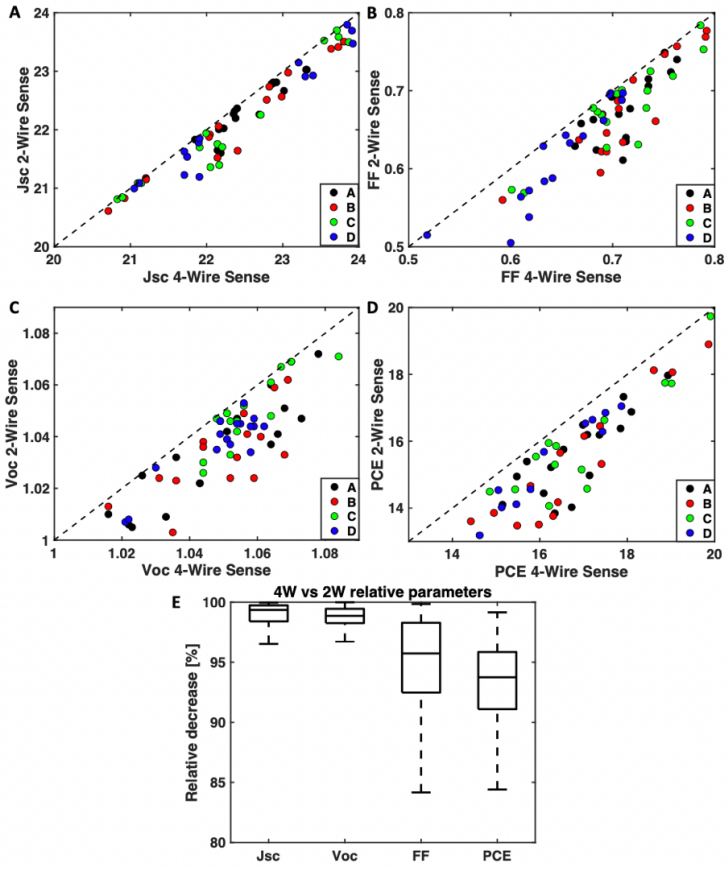

FIGURE 5 Comparison of metrics acquired using 2-wire and 4-wire sense technique. (A) J_{SC} (B) Fill Factor, (C) V_{OC} and (D) PCE of four different batches of 16 solar cells each (A, B, C, D). The diagonal line represents an equal measurement. (E) Provides relative summary of parameter decrease. A reduced standard deviation on the FF obtained by the automated measurement demonstrates the superior reliability of the measurements made with minimum human interaction. We attribute the reduced performance of the manual measurement to the sum of several minor errors, such as misalignments between the shadow mask and the electrode, and non-perpendicularity between the the sample and the incoming light. In addition, the lack of N_2 cooling and longer exposure to humidity and light, may contribute to slight degradation prior to the measurement.14-15, 17, 35

3 | CONCLUSIONS

In our work, we have developed a high-throughput solar simulator based system for perovskite solar cells for rapid combinatorial screening. This high-throughput solar cell characterization system is capable of performing measurements with high accuracy and allows for excellent versatility in terms of measurement protocols. The system provides rapid and reliable research-scale characterization for perovskite solar cells and other emerging solar cell technologies. Combined with the pre-patterned FTO substrate these automatic features can significantly increase the daily output of any research laboratory. We have shown the benefits of a 4-wire sense method for measuring perovskite solar cells, and its impact on the photovoltaic performance parameters. The system tackles commonly known issues found when measuring hysteretic PSCs and can potentially set a benchmark for PCS measurement protocols. We have demonstrated that by automating the solar simulator, we can potentially reduce the discovery time of novel perovskite materials. The high-throughput scanning improves the productivity of perovskite research laboratories, and removes human error by employing a systematic and repeatable method of characterization of PSCs.

Acknowledgements

The authors are grateful for the financial support by the Australian Research Council (ARC) ARC Centre of Excellence in Exciton Science (ACEx). The authors are grateful for the financial support by the Australian Research Council (ARC) discovery project (DP160104575), the Australian Centre for Advanced Photovoltaics (ACAP), the Australian Renewable Energy Agency, and the ARC Centre of Excellence in Exciton Science (ACEx:CE170100026). This work was performed in part at the Melbourne Centre for Nanofabrication (MCN) in the Victorian Node of the Australian National Fabrication Facility (ANFF). D.P.M acknowledges financial support from the Australian Centre for Advanced Photovoltaics (ACAP).

Conflict of interest

No conflict of interest has been declared by the author(s).

Supplementary Information

The photocurrent response is measured during a voltage sweep from short circuit to open circuit (forward) and back to short circuit (reverse). The maximum power point (MPP) is the maximum power produced (P = V x I) and is used to determine the PCE. However, in contrast to conventional semiconductor based devices, hybrid perovskites and perovskite-like materials demonstrate a severe hysteresis, a strong variation of *J-V* curve between forward and reverse scan direction during *J-V* sweeps, which complicates determination of the true MPP and PCE.36

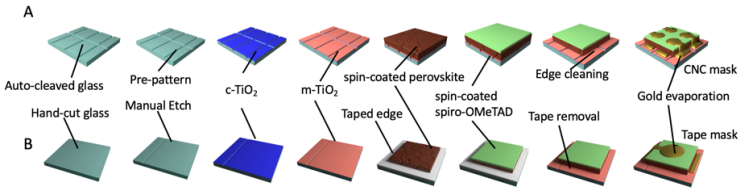

S1: Typical single cell substrate compared with our new multi-cell design fabrication steps. The new design process assures precise alignment and increases the number of cells per substrate, increasing the throughput of device fabrication by factor of about. (A) Old design requires researcher to manually cut, etch and mask to produce the device (B) Custom-fabricated precision-cut glass with machine pre-patterned etch lines, the substrate is placed inside the spray jig, after the spin coating the substrates are placed inside the evaporation jig.

To achieve that researcher has to remove conductive oxide somehow; the patterning is achieved using low power laser etching or chemical etching. Such substrates then get cleaned in staining jars and are immediately covered with electron transporting layer (ETL). Then next step is to mask areas that will be later used as contacting terminals with the tape and spin-coat the sample with perovskite precursor solution and hole transporting layer (HTL) with intermittent drying and annealing steps. Later on, the tape is removed in order to evaporate electrodes. The ultimate fabrication step is to deposit metal contacts, the substrate is masked using adhesive tape and the metal electrode layer is evaporated (see Fig.1A). A complete device is characterized using manually-aligned aperture mask to define the area exposed to sunlight. A very common procedure to measure the devices is to manually clip the two electrodes of the solar cell and illuminate the cell. However, the clips can damage the electrodes, typically a very thin (100 nm) layer of metal and/or make poor electrical contact. An alternative method is to solder wires to the electrodes which provide excellent contact. However, this process can heat the local area to temperatures in excess of 150 °C, which can induce damage or local structural/chemical changes in the device.37-39 It is obvious that such methods are very time-consuming for routine and systematic analysis and/or add undesired series resistances to the electrical measurements. Furthermore, by maintaining the exact distance between the light source and the measured cell, using a custom-designed solar simulator holder, aluminium extrusions for the x-y stage, along with a 3D printed chamber (Melbourne Centre for Nanofabrication, 16 µm feature precision), we assured perpendicularity between the incoming light and the substrates.

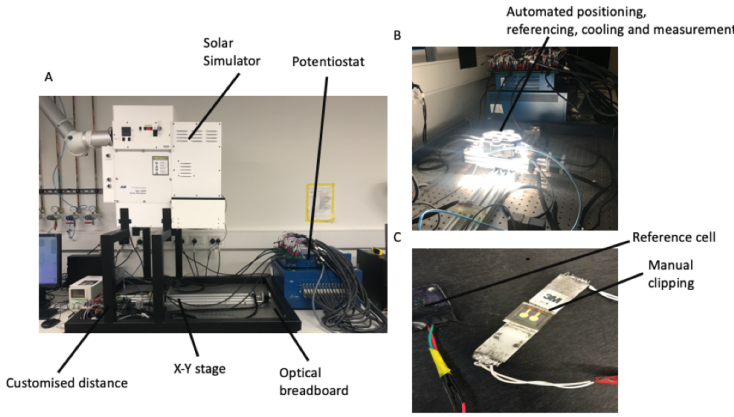

S2: The high-throughput solar cell characterization system. A) Picture of our system. B) Measurement in action using our automated method C) Picture of old style manual measurement approach.

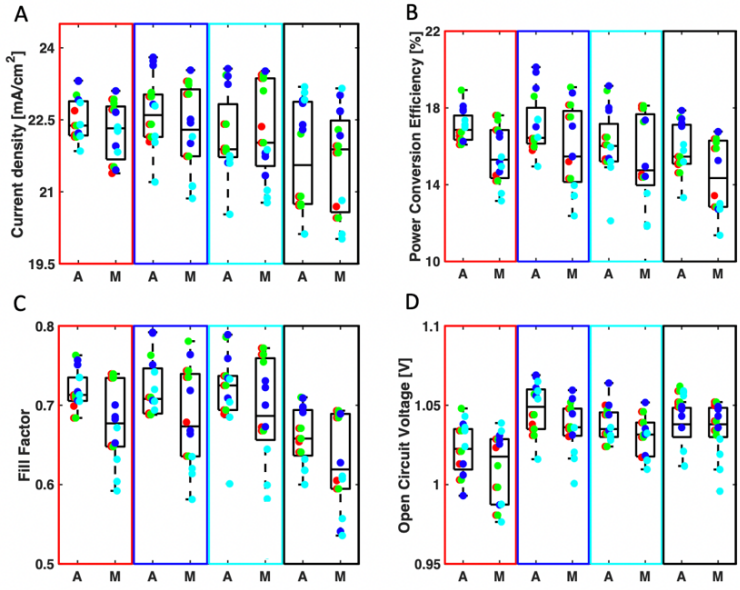

S3: The statistics of the photovoltaic parameters extracted from 4 batches of 16 cells measured using new automated technique and old manual. The automated measurement resulted in overall superior values for all parameters with reduced deviations; Champion cell: J_{SC} = 23.79 ± 0.01 mA/cm^2, V_{OC} = 1.07 ± 0.01 V, FF = 0.79 ± 0.01 and PCE = 20.12 ± 0.05 % compared to the manual mode; J_{SC} = 23.52 ± 0.01 mA/cm^2, V_{OC} = 1.06 ± 0.01 V, FF = 0.78 ± 0.01 and PCE = 19.75 ± 0.05 %.

The algorithm automatically processes the measurements and, by using the mask area input by the user, it provides an output file with the calculated photovoltaic parameters V_{OC}, J_{SC}, FF and PCE, using the equations commonly found in literature12, 14, 29, 40, readily used for further data analysis. The summary file has the batch code number, RAW

file with all measurements, graphical representation of immediate plots (less data points). The user has real-time option to observe formation of the plots (*J-V*, constant bias voltage stability and MPPT).

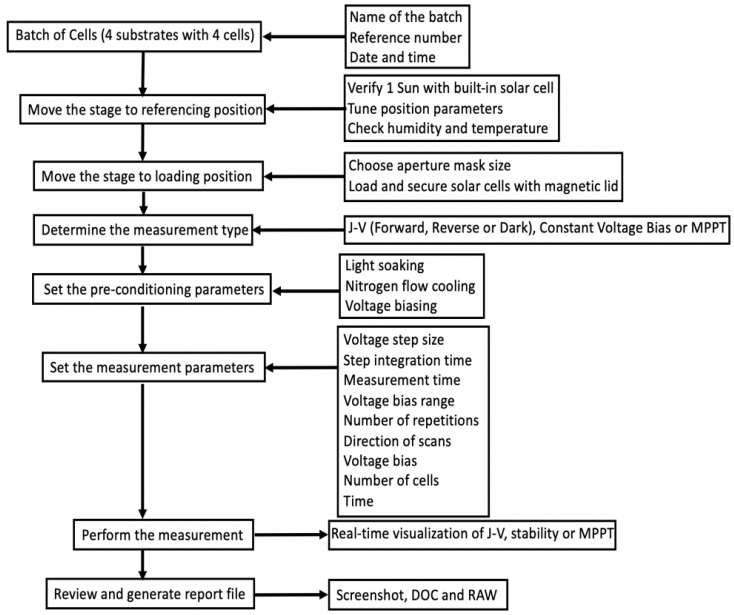

S4: Open-style protocol algorithm implemented in our software. It is designed to increase high-throughput and allow user to quickly adjust own parameters of the measurement whilst maintaining reproducing the same measurement conditions and track any changes that can occur during the measurement.

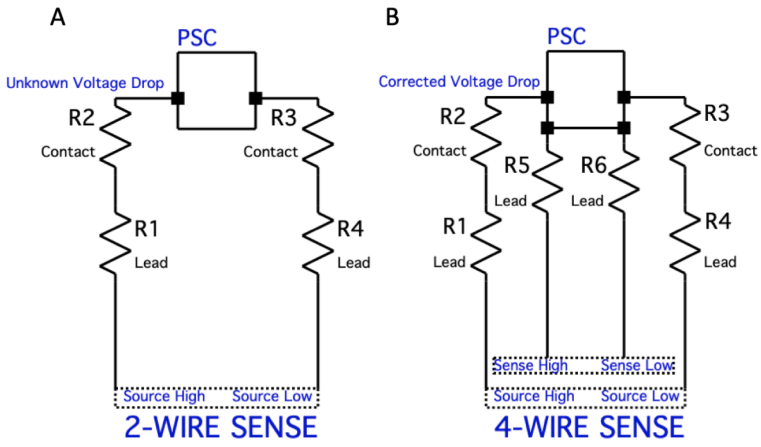

S5: The mechanism of 2WS and 4WS measurements. A) The total series resistance remains unknown, the contact resistance depends on contact between measurement probe and PSC electrode and may vary each time the device is clamped or placed in the jig. Overall, the resistance depends on the condtion of an electrode and surrounding conditions (temperature). B) Additional connections (Sense High and Sense Low) use high impedance (low current, pA) to sense the voltage drop at the test lead to PSC contact. It bypasses the voltage drops caused by the test leads and contacts, hence the voltage measured is a real photovoltage originating from PSC.

References

1. NREL Best Research-Cell Efficiency Chart. (https://www.nrel.gov/pv/cell-efficiency.html.

2. Eames, C.; Frost, J. M.; Barnes, P. R. F.; O'Regan, B. C.; Walsh, A.; Islam, M. S., Ionic transport in hybrid lead iodide perovskite solar cells. Nature Communications 2015, 6 (1), 7497.

3. Habisreutinger, S. N.; Noel, N. K.; Snaith, H. J., Hysteresis Index: A Figure without Merit for Quantifying Hysteresis in Perovskite Solar Cells. ACS Energy Letters 2018, 3 (10), 2472-2476.

4. Unger, E. L.; Hoke, E. T.; Bailie, C. D.; Nguyen, W. H.; Bowring, A. R.; Heumüller, T.; Christoforo, M. G.; McGehee, M. D., Hysteresis and transient behavior in current–voltage measurements of hybrid-perovskite absorber solar cells. Energy Environmental Science 2014, 7 (11), 3690-3698.

5. Snaith, H. J.; Abate, A.; Ball, J. M.; Eperon, G. E.; Leijtens, T.; Noel, N. K.; Stranks, S. D.; Wang, J. T.-W.; Wojciechowski, K.; Zhang, W., Anomalous Hysteresis in Perovskite Solar Cells. The Journal of Physical Chemistry Letters 2014, 5 (9), 1511-1515.

6. Pellet, N.; Giordano, F.; Ibrahim Dar, M.; Gregori, G.; Zakeeruddin, S. M.; Maier, J.; Grätzel, M., Hill climbing hysteresis of perovskite-based solar cells: a maximum power point tracking investigation. Progress in Photovoltaics: Research and Applications 2017, 25 (11), 942-950.

7. Chen, C.-Y.; Chang, J.-H.; Chiang, K.-M.; Lin, H.-L.; Hsiao, S.-Y.; Lin, H.-W., Perovskite Photovoltaics for Dim-Light Applications. Advanced Functional Materials 2015, 25 (45), 7064-7070.

8. Tress, W.; Domanski, K.; Carlsen, B.; Agarwalla, A.; Alharbi, E. A.; Graetzel, M.; Hagfeldt, A., Performance of perovskite solar cells under simulated temperature-illumination real-world operating conditions. Nature Energy 2019, 4 (7), 568-574.

9. Surface, S. T. f. R. S. S. I. D. N. a. H. o. T. ASTM G173 - 03(2008). http://www.astm.org/cgi-bin/resolver.cgi?G173.

10. Testing, S. S. f. S. S. f. T. P. ASTM E927 - 10. http://www.astm.org/cgi-bin/resolver.cgi?E927.

11. Zimmermann, E.; Ehrenreich, P.; Pfadler, T.; Dorman, J. A.; Weickert, J.; Schmidt-Mende, L., Erroneous efficiency reports harm organic solar cell research. Nature Photonics 2014, 8, 669.
12. Rakocevic, L.; Ernst, F.; Yimga, N. T.; Vashishtha, S.; Aernouts, T.; Heumueller, T.; Brabec, C. J.; Gehlhaar, R.; Poortmans, J., Reliable Performance Comparison of Perovskite Solar Cells Using Optimized Maximum Power Point Tracking. Solar RRL 2019, 3 (2), 1800287.
13. Moulé, A. J.; Meerholz, K., Morphology Control in Solution-Processed Bulk-Heterojunction Solar Cell Mixtures. Advanced Functional Materials 2009, 19 (19), 3028-3036.
14. Zimmermann, E.; Wong, K. K.; Müller, M.; Hu, H.; Ehrenreich, P.; Kohlstädt, M.; Würfel, U.; Mastroianni, S.; Mathiazhagan, G.; Hinsch, A.; Gujar, T. P.; Thelakkat, M.; Pfadler, T.; Schmidt-Mende, L., Characterization of perovskite solar cells: Towards a reliable measurement protocol. APL Materials 2016, 4 (9), 091901.
15. Dunbar, R. B.; Duck, B. C.; Moriarty, T.; Anderson, K. F.; Duffy, Noel W.; Fell, C. J.; Kim, J.; Ho-Baillie, A.; Vak, D.; Duong, T.; Wu, Y.; Weber, K.; Pascoe, A.; Cheng, Y.-B.; Lin, Q.; Burn, P. L.; Bhattacharjee, R.; Wang, H.; Wilson, G. J., How reliable are efficiency measurements of perovskite solar cells? The first inter-comparison, between two accredited and eight non-accredited laboratories. Journal of Materials Chemistry A 2017, 5 (43), 22542-22558.
16. Christians, J. A.; Manser, J. S.; Kamat, P. V., Best Practices in Perovskite Solar Cell Efficiency Measurements. Avoiding the Error of Making Bad Cells Look Good. The Journal of Physical Chemistry Letters 2015, 6 (5), 852-857.
17. Dunbar, R. B.; Moustafa, W.; Pascoe, A. R.; Jones, T. W.; Anderson, K. F.; Cheng, Y.-B.; Fell, C. J.; Wilson, G. J., Device pre-conditioning and steady-state temperature dependence of CH3NH3PbI3 perovskite solar cells. Progress in Photovoltaics: Research and Applications 2017, 25 (7), 533-544.
18. Mundhaas, N.; Yu, Z. J.; Bush, K. A.; Wang, H.-P.; Häusele, J.; Kavadiya, S.; McGehee, M. D.; Holman, Z. C., Series Resistance Measurements of Perovskite Solar Cells Using Jsc–Voc Measurements. Solar RRL 2019, 3 (4), 1800378.
19. O'Regan, B. C.; Barnes, P. R. F.; Li, X.; Law, C.; Palomares, E.; Marin-Beloqui, J. M., Optoelectronic Studies of Methylammonium Lead Iodide Perovskite Solar Cells with Mesoporous TiO2: Separation of Electronic and Chemical Charge Storage, Understanding Two Recombination Lifetimes, and the Evolution of Band Offsets during J–V Hysteresis. Journal of the American Chemical Society 2015, 137 (15), 5087-5099.
20. Measurements, P. Multichannel Solar Characterization Systems. http://www.pvmeasurements.com/Products/I-V-Measurements/solar-cell-i-v-data-acquisition-system.html.
21. Pellet, C. S. N. Multichannel Solar Characterization Setup. contact@candlelight-systems.com.
22. Ossila Solar characterization System. https://www.ossila.com/products/solar-cell-iv-test-system?variant=13633049100384.
23. Instruments, N. 1-channel SMU. http://www.ni.com/en-au/support/model.pxi-4130.html http://www.ni.com/example/30918
24. Snaith, H. J., How should you measure your excitonic solar cells? Energy Environmental Science 2012, 5 (4), 6513-6520.
25. Ito, S.; Nazeeruddin, M. K.; Liska, P.; Comte, P.; Charvet, R.; Péchy, P.; Jirousek, M.; Kay, A.; Zakeeruddin, S. M.; Grätzel, M., Photovoltaic characterization of dye-sensitized solar cells: effect of device masking on conversion efficiency. Progress in Photovoltaics: Research and Applications 2006, 14 (7), 589-601.
26. Kiermasch, D.; Gil-Escrig, L.; Bolink, H. J.; Tvingstedt, K., Effects of Masking on Open-Circuit Voltage and Fill Factor in Solar Cells. Joule 2019, 3 (1), 16-26.
27. Chen, Q.; Chen, L.; Ye, F.; Zhao, T.; Tang, F.; Rajagopal, A.; Jiang, Z.; Jiang, S.; Jen, A. K. Y.; Xie, Y.; Cai, J.; Chen, L., Ag-Incorporated Organic–Inorganic Perovskite Films and Planar Heterojunction Solar Cells. Nano Letters 2017, 17 (5), 3231-3237.
28. International, A., ASTM E927-10. West Conshohocken, PA, 2010.
29. Shrotriya, V.; Li, G.; Yao, Y.; Moriarty, T.; Emery, K.; Yang, Y., Accurate Measurement and Characterization of Organic Solar Cells. Advanced Functional Materials 2006, 16 (15), 2016-2023.

30. Wang, Y.; Liu, X.; Zhou, Z.; Ru, P.; Chen, H.; Yang, X.; Han, L., Reliable Measurement of Perovskite Solar Cells. Advanced Materials 2019, 0 (0), 1803231.
31. Zhao, C.; Chen, B.; Qiao, X.; Luan, L.; Lu, K.; Hu, B., Revealing Underlying Processes Involved in Light Soaking Effects and Hysteresis Phenomena in Perovskite Solar Cells. Advanced Energy Materials 2015, 5 (14), 1500279.
32. Xu, X.; Shi, J.; Wu, H.; Yang, Y.; Xiao, J.; Luo, Y.; Li, D.; Meng, Q., The influence of different mask aperture on the open-circuit voltage measurement of perovskite solar cells. Journal of Renewable and Sustainable Energy 2015, 7 (4), 043104.
33. Saliba, M.; Correa-Baena, J.-P.; Wolff, C. M.; Stolterfoht, M.; Phung, N.; Albrecht, S.; Neher, D.; Abate, A., How to Make over 20% Efficient Perovskite Solar Cells in Regular (n–i–p) and Inverted (p–i–n) Architectures. Chemistry of Materials 2018, 30 (13), 4193-4201.
34. Fu, F.; Feurer, T.; Weiss, Thomas P.; Pisoni, S.; Avancini, E.; Andres, C.; Buecheler, S.; Tiwari, Ayodhya N., High-efficiency inverted semi-transparent planar perovskite solar cells in substrate configuration. Nature Energy 2016, 2, 16190.
35. Jena, A. K.; Kulkarni, A.; Miyasaka, T., Halide Perovskite Photovoltaics: Background, Status, and Future Prospects. Chemical Reviews 2019, 119 (5), 3036-3103.
36. Chen, B.; Yang, M.; Priya, S.; Zhu, K., Origin of J–V Hysteresis in Perovskite Solar Cells. The Journal of Physical Chemistry Letters 2016, 7 (5), 905-917.
37. Ke, J. H.; Yang, T. L.; Lai, Y. S.; Kao, C. R., Analysis and experimental verification of the competing degradation mechanisms for solder joints under electron current stressing. Acta Materialia 2011, 59 (6), 2462-2468.
38. Han, Y.; Meyer, S.; Dkhissi, Y.; Weber, K.; Pringle, J. M.; Bach, U.; Spiccia, L.; Cheng, Y.-B., Degradation observations of encapsulated planar CH3NH3PbI3 perovskite solar cells at high temperatures and humidity. Journal of Materials Chemistry A 2015, 3 (15), 8139-8147.
39. Lanin, V. L., Ultrasonic soldering in electronics. Ultrasonics Sonochemistry 2001, 8 (4), 379-385.
40. Schwander, D. In Dynamic Solar Cell Measurement Techniques: New Small Signal Measurement Techniques, Space Power, May 01, 2002; 2002; p 603.
41. N. Park, H. Segawa, Research Direction toward Theoretical Efficiency in Perovskite Solar Cells, ACS Photonics, 2018, Vol. 5, Issue 8, p 2970-2997
42. Y. Li et al., “High-throughput computational design of organic–inorganic hybrid halide semiconductors beyond perovskites for optoelectronics”, Energy Environ. Sci., 2019, 12, 2233-2243
43. S. Sun et al., “Accelerated Development of Perovskite-Inspired Materials via High-Throughput Synthesis and Machine-Learning Diagnosis”, Volume 3, Issue 6, 19 June 2019, Pages 1437-1451
44. M. Saliba et al., “Polyelemental, Multicomponent Perovskite Semiconductor Libraries through Combinatorial Screening”, Adv. Energy Mater. 2019, 9, 1803754
45. Y. Cai et al., “High-throughput Computational Study of Halide Double Perovskite Inorganic Compounds”, Chem. Mater. 2019, 31, 15, 5392-5401
46. S. Chen et al., “Accelerating the Screening of Perovskite Compositions for Photovoltaic Applications through High-Throughput Inkjet Printing”, Adv. Funct. Mater. 2019, 29, 1905487
47. J. Li et al., “High-Throughput Combinatorial Optimizations of Perovskite Light-Emitting Diodes Based on All-Vacuum Deposition”, Adv. Funct. Mater. 2019, 29, 1903607 48. Green, M. A. (1981). Solar cell fill factors: General graph and empirical expressions. Solid-State Electronics, 24(8), 788–789. doi:10.1016/0038-1101(81)90062-9

ORIGINAL ARTICLE

Journal Section

High-Throughput Characterization of Perovskite Solar Cells for Rapid Combinatorial Screening

Maciej Adam Surmiak[1*] | Tian Zhang[2†] | Jianfeng Lu[2†] | Kevin James Rietwyk[2†] | Sonia Ruiz Raga[2†] | David Patrick McMeekin[2†] | Udo Bach[2]

[1]Department of Chemical Engineering, Monash University, Victoria 3800, Australia

[2]ARC Centre of Excellence for Exciton Science, Monash University, Victoria 3800, Australia

Correspondence
Professor Udo Bach, Chemical Engineering, Monash University, Clayton, Victoria, 3800, Australia
Email: udo.bach@monash.edu

Present address
[†]Chemical Engineering, Monash University, Clayton, Victoria, 3168, Australia

Funding information
The authors are grateful for the financial support of this work by the Australian Centre for Advanced Photovoltaics (ACAP), the Australian Renewable Energy Agency and the ARC Centres of Excellence in Exciton Science (ACEX; CE170100026)

In order to discover the ideal perovskite material for solar cell application, a large parameter space (composition, surrounding condition, fabrication technique etc.) must first be explored. Hence, screening this parameter space using a rapid combinatorial screening approach could drastically speed-up the rate of discovery. During the last decade, these discoveries and optimization processes of perovskite materials have been achieved using simple lab-scale deposition techniques and characterization methods, resulting in a substantial time-consuming process, slowing the rate of progress in field of photovoltaics. Thus, the benefits of developing fully-automated, high-throughput characterization techniques become apparent. In this paper, we detail a high-throughput solar cell testing system that enables parallel, real-time and comprehensive measurements, allowing for 16 solar cells to be characterized simultaneously. We show the importance of measurement reproducibility, condition verification and structured data post-processing.

KEYWORDS
Perovskite Solar Cell, Characterization, High-throughput

Abbreviations: ARC, Australian Research Council; ACEX, Australian Centre of Excellence in Exciton Science

[*]Equally contributing authors.

1 | INTRODUCTION

In the past decade, there has been a drastic upheaval in the research of photovoltaics with the introduction of solution-processed solar cells, particularly inorganic-organic hybrid lead halide perovskite materials. Perovskite materials have a general ABX_3 chemical formula, where A is a cation, B a divalent metal ion, and X a halide. Moreover, by adjusting the chemical composition of the A-site cation, commonly, (methylammonium, and formamidinium, or caesium), the B-site metal cation (lead or tin) or the X-site anions (iodide, bromide, chloride) we can fine-tune the optoelectronic properties of this novel semiconductor. Perovskite solar cells (PSCs) have achieved significant power conversion efficiencies that are currently competing with commercially available solar cells.1 Their performance continuously improved over the past decade, reaching a certified power conversion efficiency (PCE) of 25.2%1, rivalling the all-time champion silicon solar cells (SCs) with record efficiencies of 26.1%1. However, the characterization of PSC is non-trivial due to their ionic movement within the material, resulting in a range of transient behaviors when attempting to measure their performance.2 Due to this ionic movement within the film when a voltage bias is applied, a hysteric behavior is observed during the measurement of the current-voltage (*J-V*)3-5 curve. To eliminate the effect of ionic motion when determining the true performance of the device, a maximum power point tracking (MPPT) technique is preferred over a *J-V* scan.6 Furthermore, to mitigate the effect of heating caused by 1 Sun illumination, which can reach 35-40°C, the device is held at 25°C using a nitrogen gas flow7-8, when illuminated with a spectral irradiance of AM 1.5G and a 1000 W/m^2 power density using a lamp (xenon, quartz tungsten halogen, metal halide or light-emitting diode)9-10 and area-defining mask. The ionic behavior of lead halide perovskites causes a hysteric behavior in the *J-V* curve, depending on scan parameters such as: scan direction, speed, settling time and bias voltage range. These devices also demonstrate severe memory-like effects, where the performance is altered by past measurement such as: light soaking, applied voltage bias, storage under specific atmospheres and temperatures. Recently, Zimmermann *et al*., Pellet *et al*. and Rakocevic *et al*. addressed the complex challenges in reliability of the measurements.6, 11-12 Perovskite laboratories around the world have their own ad-hoc *J-V* measurement protocols, thus causing ambiguity when reporting the true performance of the solar.12-16 11 Despite the aforementioned issues, *J-V* scans still remain a key characterization tool amongst the perovskite research community. The most reliable method for measuring a *J-V* curve, is the dynamic *J-V* curve, where the current-density for each voltage point is measured long enough to demonstrate stable current).17 Although this method is highly accurate and only requires a sweep in a single direction, this approach takes longer to perform compared to a conventional *J-V* curve (where, the extracted current is stabilized over a period of time determined by the user. Therefore, the generally agreed best approach to determine the stabilised PCE is to track the evolution of the extracted current at maximum power point voltage over the course of typically 1-10 minutes. Similarly, to obtain a stabilised measurement of the short-circuit current density (J_{SC}), and open-circuit voltage V_{OC}, a time-depend approach can be utilised. Another approach to obtain a stabilized *J-V*, involves repeating the measurement of the *J-V* curve until the curve stabilizes, thus, accounting the impact of "light-soaking". 16, 18-19 However, each method has their own shortcomings, hence, to account for the fluctuation in maximum power point (V_{MPP}) over time, while also minimizing the measurement time, a maximum power point tracking (MPPT) is viable approach as a characterising method. Dunbar *et al*. recently reported an inter-laboratory comparison on the measurement of perovskite solar cells that highlights the variability in measurement protocol across 10 laboratories.15 One of the key findings was that the variability in measured PCE for each laboratory was primarily determined by light and voltage pre-conditioning, electrical measurement protocol and inaccuracies in estimating the cell active area. The manual handling of the devices during the fabrication and characterization and the arbitrary choice of measurement parameters contribute to difficulties when comparing PCE from lab-to-lab. Therefore, in order to bolster research outcomes, it is preferred to automatize and standardize such routine electrical characterizations and develop MPPT algorithms to

accurately report PCE. Only a few commercial solar cell measurements systems are available today, however, they usually do not achieve all three desired requirements for PSC research: (i) customisation of measurement parameters and protocols, (ii) simultaneous measurement of several devices and (iii) a sample holder to precisely overlap the aperture mask with the counter electrodes. Due to lack of versatile commercial instruments crafted specifically for perovskite solar cells, many researchers decide to design their own characterization set-ups, based on programmable source-measure units (NI, Ossila, Keysight or Keithley). Some of the commercial products offer automated computation of key characterization parameters commonly found across solar cell research, however, these parameters are not necessarily tailored towards the specific needs of PSCs, such as light and bias pre-conditioning, or versatility in selecting *J-V* parameters such dwell time or scan speed to mitigate the impact of the hysteretic behavior found in PSC. These measurement instruments were designed to cater to the for solid state solar cell industry, which do not exhibit strong transient behavior when being measured. Here we present a systematic study using a versatile state-of-the-art high-throughput solar cell characterization system, capable of testing up to 16 solar cells simultaneously, while maintain a high level of reproducibility. We demonstrate the advantages of the system in terms of accuracy, speed and reproducibility, with our results captured in less than one tenth of the measurement time compared to conventional approaches. We believe that this system will provide a valuable guidance for researchers, when characterizing PSC with hysteretic behavior and consequently will play an important role in developing future measurement system for the photovoltaics (PV) industry.

2 | RESULTS AND DISCUSSION

At research-scale, solar cell devices are generally fabricated on individual substrates of area less than 5 cm^2 due to size limitations posed by laboratory equipment, and in order to reduce research costs. The laboratory fabrication process for PSC test cells typically involves the manual cutting of transparent conductive oxides (TCO) substrates by hand tools, which results in poorly controlled substrate shapes and sizes. The manual cutting and patterning require extra care and extensive cleaning and despite efforts of being precise manual cutting causes significant glass size difference (± 1 - 3 mm) making the use of precise jig and masking impossible. In order to address these bottlenecks for high throughput solar cell research, we combine a number of techniques to reduce the manual handling using a jig (positioning device) based fabrication (Supplementary Information, S1). Firstly, we increased the number of solar cells per substrate. The old substrates were diced by hand from 100x100 mm of fluorine-doped tin oxide (FTO, < 14 Ω/sq.) to ± 25 x 25 mm pieces. New ones are commercially ordered as precision-cut, pre-patterned pieces covered with a thin film of fluorine-doped tin oxide (FTO, < 10 Ω/sq.). For that, we have designed a new substrate architecture that can contain four individual solar cells electrically isolated from each other (see Fig. 1A). Custom-made, precision-cut, pre-patterned FTO glass substrate (accuracy ± 0.15 mm) were sourced from Latech Scientific Supply Pte Ltd (Singapore). The glass is cleaned in specially ordered trays which are placed in ultrasonic baths. Cleaned substrates are dried and placed in precisely milled jig. The automated way of spraying TiO_2 therefore allows minimizing discrepancy of layer thickness and quality from batch to batch. The ETL covered substrates are therefore transported to glovebox where spin coating of perovskite precursor solution and HTL is performed. Later on, the substrates are placed in another precisely milled jig in order to evaporate Au electrodes making the alignment and masking procedure completely redundant, ensuring the same position of the electrodes across entire batch of solar cells. We have encompassed in the design that the tolerance build-up between each commercially purchased substrate (up to ± 0.15 mm), position in the measurement pocket (± 0.016 mm) and evaporation plate (± 0.01 mm) can negatively influence results, so therefore we have designed the connection printed circuit board (PCB) accordingly. The pin rows are positioned in

the middle of 2 mm wide contact electrode areas; thus, the connection is always established. We highlighted the fabrication differences in fabrication step in Tab.1.

TABLE 1 Comparison between fabrication steps of new and old design solar cell.

Variables	Alignment required	Old method	New method
Glass cutting	Y	Hand scribe and cut	Precision laser cut (± 0.15 mm)
Pattern etching	Y	Manual	Laser pattern (± 0.001 mm)
Compact TiO_2	Y	Manual	Automated spray inside of jig*
Mesoporous TiO_2	N	Jig not required	Jig not required
Perovskite	N	Jig not required	Jig not required
Spiro-OMeTAD	N	Jig not required	Jig not required
Edge removal	Y	Solvent cleaning	Machine buffing
Gold evaporation	Y	Tape masking	CNC milled jig (± 0.01mm)
Shadow mask	Y	Manually placed	Guided and magnet-clamped

*jig - device used for positioning.

2.1 | Methodology

We designed a custom-made sample holder (Fig. 1D) that allows for the simultaneous measurement of four substrates, containing four solar cells. The holder allows for precise alignment between the aperture mask and the active area, further details on the sample mounting are presented in Fig.1B,C. In addition, the holder has built-in sensors for temperature and relative humidity, as well as a Si photodiode reference cell with KG5 filter. The chamber also has ports and lines for N_2 gas circulation, directed onto the solar cells to reduce the presence of oxygen and moisture, while simultaneously providing an active cooling during the measurement process. All sensors, photodiode and N_2 valves are communicating with the computer through a microcontroller (ATmega 2560), giving full access to the end user. The 16 solar cells are connected to a commercially available, computer controlled, 16-channel potentiostat (Bio-Logic VMP3). The holder provides electrical contact by utilising a magnetic lid to press the solar cells onto the spring loaded pins. The custom-built PCB board is mounted inside of the sample to provide good contact connection between the pin and electrode. We have used a two-fold-redundancy system to always achieve electrical contact connection. The sample holder is mounted on a motorized two-axis (x-y) stage that is connected to the PC through a second microcontroller. The moving stage allows the light intensity to be mapped using the reference Si solar cell, then the solar cells are placed in the region with greatest illumination uniformity; this will be explained in detail in Section 2.3. Moreover, the x-y moving stage could potentially host several sample holders to further increase the throughput of the solar simulator by sequentially measuring batches of 16 devices. The motorized stage is aligned with a commercial solar simulator (Abet Technologies Sun 3000 class AAA). The solar simulator is equipped with a software-operated built-in programmable light shutter wired to one of the microcontrollers. Finally, the system is controlled by a custom-made piece of LabView software; further details on the characteristics of the protocol are provided in Section 2.3; for picture see Supplementary Information, S2.

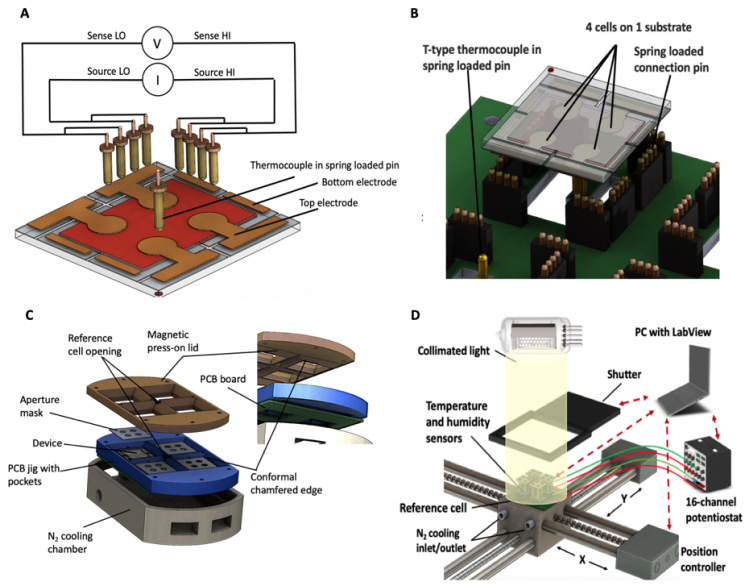

FIGURE 1 Schematic diagram of the high-throughput solar cell characterization system. (a) A schematic showing a custom-designed pre-patterned FTO substrate that is being probed in a 4-wire sense configuration with spring-loaded pins. (b) Close up of a single substrate slot, where each cell is connected with 8 spring loaded pins, and measured with a 4-wire sense technique. (c) Single measurement module consists of positioning jig where the substrates are mounted, the design allows the room for a thin 0.08 mm black dyed stainless-steel apertures masks. The masks are pressed against the solar cells by a magnetic force and the chamfered protrusion guides the magnetic lid in place restricting the movement of the cells and ensuring electrical connection between solar cells and spring-loaded probes. (d) Sample holder consists of a printed circuit-board (PCB) equipped with spring loaded gold pins that provide electrical connection between the 16 solar cells and the potentiostat. The red dashed lines denote communication routes between PC and system parts.

The devices were made in the following way, the substrates are cleaned using Hellmanex® 2% DI water solution, DI water, solvents: acetone, ethanol, isopropanol, respectively and place in an ultrasonic bath for 15 minutes. Onto the FTO a compact layer 10-20 nm of TiO_2 is deposited using spray-pyrolysis. For this, 1 mL of bis(isopropoxide)-bis (acetylacetonate)titanium(IV) dissolved in 19 mL of anhydrous isopropanol at 500°C. Subsequently a mesoporous TiO_2 layer 150-200 nm was spin-coated at 4000 RPM for 20 s with a ramp of 2000 RPM/s using a 30 nm of Dyesol 30 NR-D diluted in ethanol (30 NR-D: ethanol = 1:6, wt.). After that the substrates were dried at 110°C (10 minutes), then they were annealed at 500°C (30 minutes). This was followed by preparation of perovskite films prepared entirely in a N_2 filled glove box including spin coating and annealing and preparation of the precursor solutions. Perovskite precursor solutions were produced by dissolving FAI (1.1 M (M = mole L-1), PbI_2 (1.2 M), MABr (0.22 M), $PbBr_2$ (0.24 M), and CsI (0.07 M) in anhydrous dimethylformamide (DMF):dimethyl sulfoxide (DMSO) (4:1 v/v) to achieve

a composition of $Cs_{0.05}FA_{0.79}MA_{0.16}PbI_{2.49}Br_{0.51}$ with a concentration 1.44 M. The perovskite film was fabricated by spin-coating 80 L of the perovskite precursor solution per substrate using a 2-step program: 1000 RPM for 10 s (1000RPM/s ramp), followed by 6000RPM for 20 s at (6000RPM/s ramp). Then 200 L of chlorobenzene was poured onto the spinning substrate 5 s prior to the end of the second step. The samples were annealed in the dark at 100°C (1 hour) and then allowed to cool to 25°C. After cooling, 80 L of a chlorobenzene solution containing spiro-OMeTAD (60 mM), 4-tert-butylpyridine (tBP; 198 mM), bis(trifluoromethanesulfonyl) imide (LiTFSI; 30 mM), with (1.8 mM) cobalt complex FK269(III), was spin-coated at 3000 RPM for 30 s (3000 RPM/s ramp). A gold (Au) counter-electrode (80 nm) was then deposited on the HTM layer by thermal evaporation. To minimize the possibility of having unconnected cell we used a row of 4 soft spring-loaded pins, having more pins also minimizes damaging of the 80 nm thick metal electrode. This allowed to minimize mechanical damage to the electrodes. Every solar cell is connected with 8 pins in total. To address the issue of the unwanted contact resistance and cable resistance, we implemented a 4-wire sense connection (see Fig.1A). The testing current is applied to the outer pair of contacts and the voltage is measured with the inner pair, for each electrode. The measurement performed at high impedance, thus eliminating the current and voltage drop caused by the contact resistance and the resistance of the external measuring circuit.15 To ensure precision, we designed a thin (0.08 mm) stainless steel opaque aperture mask with a laser-cut opening (0.16 cm^2 ± 0.001 cm^2), to create a precise and well-defined aperture to illuminate the device under test (DUT). Precise of fabrication of this aperture mask is essential to accurately control the active area of the illuminated device and to determine the PCE. We performed a study to establish the optimal ratio between the gold electrode and illumination mask diameter (see Fig. 2). Similarly, it has been demonstrated in Dye-sensitized Solar Cells (DSC) by Ito *et al*. (2006) that the aperture mask size in comparison to the electrode area impacted performance.25 By masking the cells we mitigate any artificial V_{OC} gains.26

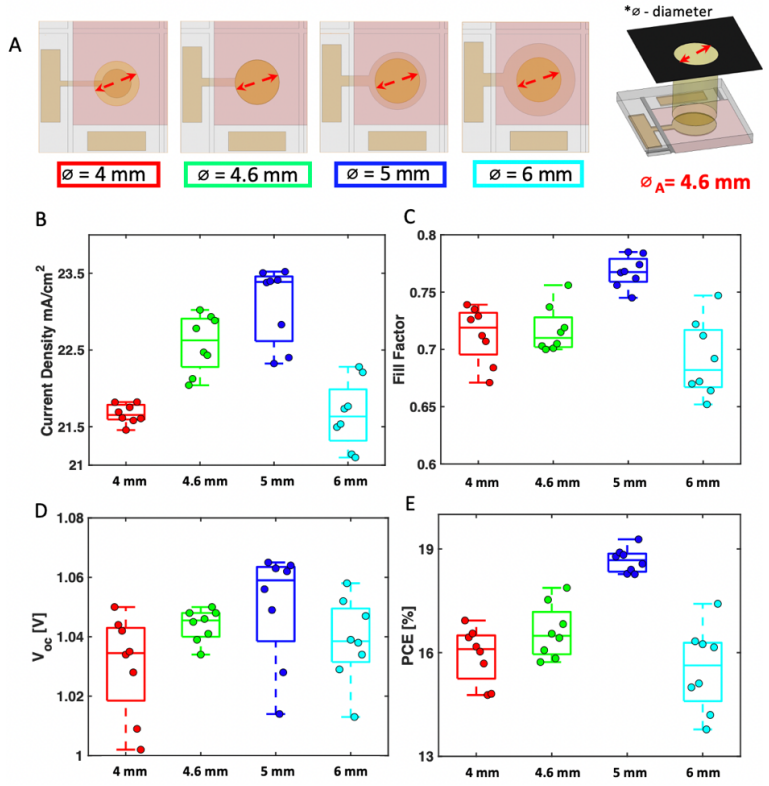

FIGURE 2 Comparison between performance of batches of 8 test cells with various gold electrode diameters (d) with fixed across perovskite. A) Fixed size aperture mask (ø) allowing only specific area to be illuminated vs various diameter of the gold electrode. B) Open circuit voltage, C) Fill factor, D) Current density, E) Power conversion efficiency.

A key concern with performing simultaneous characterization of multiple cells on a single substrate is the possibility of a crosstalk, i.e. current flow between adjacent cells, thus impacting the *J-V* measurement. Despite the wide 0.5 mm pseudo-moat separating the four cells of the patterned FTO glass substrate, lateral current leakage may potentially occur through the perovskite layer, or the HTM or ETL. In order to check for the presence of crosstalk we performed simultaneous *J-V* scans for the 4 cells, of which only two were under illumination (1 and 4) while the two others were shaded from direct illumination, as shown in Figure 3. The short-circuit current density of cells 1 and 4 exceeds 20 mA/cm², while cells 2 and 3 exhibit no significant photocurrent, much below «0.01 mA/cm^2, indicating that the design of the patterned substrate connections and masking is highly effective to impede the crosstalk, for the materials employed (i.e.$Cs_{0.05}FA_{0.79}MA_{0.16}PbI_{2.49}Br_{0.51}$, TiO_2, and Li-TFSI-doped spiro-OMeTAD).18, 27

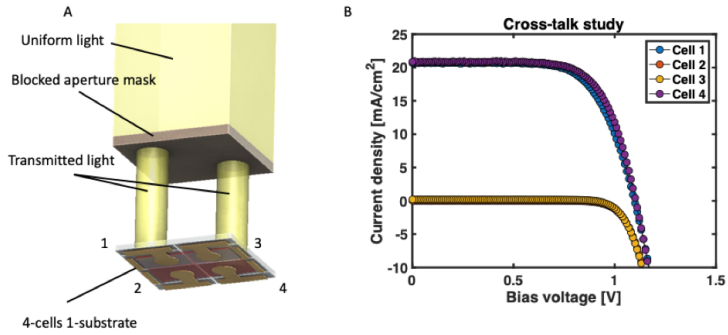

FIGURE 3 Evaluation of cross-talk between solar cells co-located on the same substrate. A) Schematic of a substrate with four solar cells during current-voltage measurement with cells 1 and 4 exposed to illumination and 2 and 3 in the dark. The mask is precisely placed on top of the measured device. B) *J-V* curve of the four cells. The illuminated cells exhibit a voltage dependent photocurrent as expected, while the two kept in the dark exhibit no photocurrent, indicating a complete lack of cross-talk between the cells.

2.2 | Illumination and external conditions

For research purposes, solar cells are measured under a standardized light source; this enables reproducibility and comparison among laboratories around the world. A xenon lamp light sources emits an electromagnetic spectrum that closely matches the sunlight that reaches the Earth surface after correction of spectral and intensity loss caused by atmospheric gases. This is achieved by using a filter that corrects the xenon spectra to AM1.5, corresponding to a zenith angle of 48.2° and adjusting the lamp power (100 mW/cm^2). 28 The highest class of solar simulators is AAA, which fulfils strict requirements including a uniformity of irradiance of less than 2% across the region of interest and exhibit spectral agreement with the AM1.5G solar spectral of within ± 25% at any wavelength. The overall irradiance of the solar simulator is typically determined using a certified reference Si solar cell with a KG filter.24, 29-30 However, as the lamp ages, the illumination intensity may fluctuate, thus regular monitoring of the actual irradiation power density with a calibrated reference cell prior to the measurements is advisable. To this end, we have integrated a reference Si solar cell in the x-y motorised stage and a simple LabView® code, allowing the user to routinely map the illumination from the solar simulator and confirm that a 1 ± 0.02 Sun equivalent is maintained across the region of interest. An example is given in Figure 4. The program identifies the x-y coordinates for the area with less deviation to 1 Sun intensity and automatically places the sample holder under that region to proceed with the electrical measurements. This ensures a comparable light intensity for each of the cells measured simultaneously and provides a useful tool for gauging the aging on the xenon lamp.

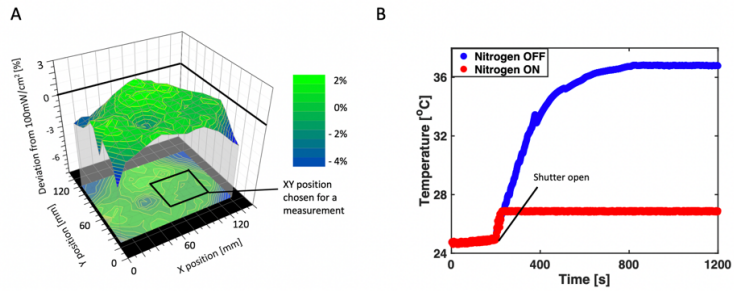

FIGURE 4 A) Spatial map of the relative solar intensity under the solar simulator. The ideal region for analysis is where the deviation is closest to 0%. B) Temperature of the substrate with and without N_2 cooling. The temperature fluctuations in presence of N_2 gas flow are smaller and the temperature after opining the shutter remains at lower level than without active cooling.

2.3 | Electrical characterization of PSCs

As we have mentioned, due to the hysteric behaviour of PSCs, we have designed the software to allow the end-user to vary each electrical parameter according to standard measurements, such as: scan direction, initial voltage, end voltage, scan rate or scan speed, the number of sampling points or voltage step and dwell time or settlement time. In addition, the following pre-conditioning options are available: set an applied voltage and/or open the shutter and light-soak for a certain time a priori to measurement, open the gas valve to purge the chamber and cool the sample before measurement. The user can test stability of the cell by setting the bias voltage and measure the extracted current of up to 16 cells simultaneously. Finally, our software can automatically track the MPP (up to 16 devices in real-time parallel algorithm) where the MPP is sampled up to every 12 seconds to ±10 mV around the previous value and obtains the real-time MPP. The widely discussed in the literature differences between MPPT evolution amongst various perovskite and carrier transport layer (CTL) prompted us to address findings as such.11-12, 14 The most importantly we do not define one and only good characterization method, but rather we implemented possibility to choose between different parameters (voltage step size, voltage dwell time, stabilized transient current test). The users can pick their own parameter set, which is specific for the measured solar cell composition. Furthermore, the user defines the light soaking and gas exposure time,31 and aperture mask area.32 (protocol details and automatically produced statistics can be found in Supplementary Information, S3 and S4) The temperature of substrates was measured before the measurement at 24.2 °C with the relative humidity of the room measured to be RH = 41.2 %. Prior to performing measurements, the solar cells are exposed to N_2 flow for 30 s. We have mapped (system has option of systematic mapping to establish the lamp aging intensity decay) the illumination area to ensure that we are under simulated air mass (AM) 1.5 solar illumination of 100 mW/cm^2. We have chosen 5 s of light soaking prior to scanning at 0 V bias voltage. The voltage was swept from -0.2 to 1.2 V at a scan speed of 80 mV/s with voltage-steps of 10 mV. An *J-V* sweep was initially performed in the dark (solar simulator shutter closed) followed by forward and reverse scans under illumination. We have performed 4 separate tests of 16 solar cells using automated and manual methods. The obtained data from these measurements is presented on Fig. 5. To demonstrate the effectiveness of the solar cell characterization system in terms of accuracy and speed, we proceed to compare the experimental results of 4 batches of 16 solar cell (batches are denoted with A, B, C, D on Fig.5), totalling 64 measurements using first the 16-channel system and comparing it to a single cell manual clipping measurement where each cell is simply connected with alligator clip. An experienced researcher requires an average of 2 min for aligning and fixing the illumination mask,

clipping the two electrodes and placing it perpendicularly to the illumination beam of the solar simulator. Afterwards, an average of 2 min is consumed for sample data entry and running the *J-V* measurement. This protocol, repeated 16 times, resulted in a total of 60 min for the manual measurements, whereas for the automated measurement the devices were mounted simultaneously measured within 5 min. This full automation designed to increase characterization speed is motivated by combinatorial screening in order to discover and optimize novel perovskite compounds. Saliba *et al*. presented a positively trending correlation between the number of fabricated and characterized cells and their overall performance.33 On average, a research laboratory can produce daily 10-20 cells per person hence by having an automatized measurement, we can not only speed up the characterization, but as well make sure that the fabricated devices are treated equally and none of them needs to wait in queue in order to be characterized. As aforementioned, the negative impact of external conditions can significantly degrade the cells and potentially derail the research of a prospecting composition/material/architecture of PSC. The test cells and hence the photocurrents are typically small. In our case I_{SC} < 4 mA. It is often perceived that the 4-wire sense is not required, when measuring such small currents. All data points come to sit underneath the diagonal indicative of a systematic underestimation of PV performance parameters when using 2WS. In average this resulted in an underestimation of the PCE of 1-2%. This highlights the importance of using 4WS when measuring PSC test cells using contact pins. 34

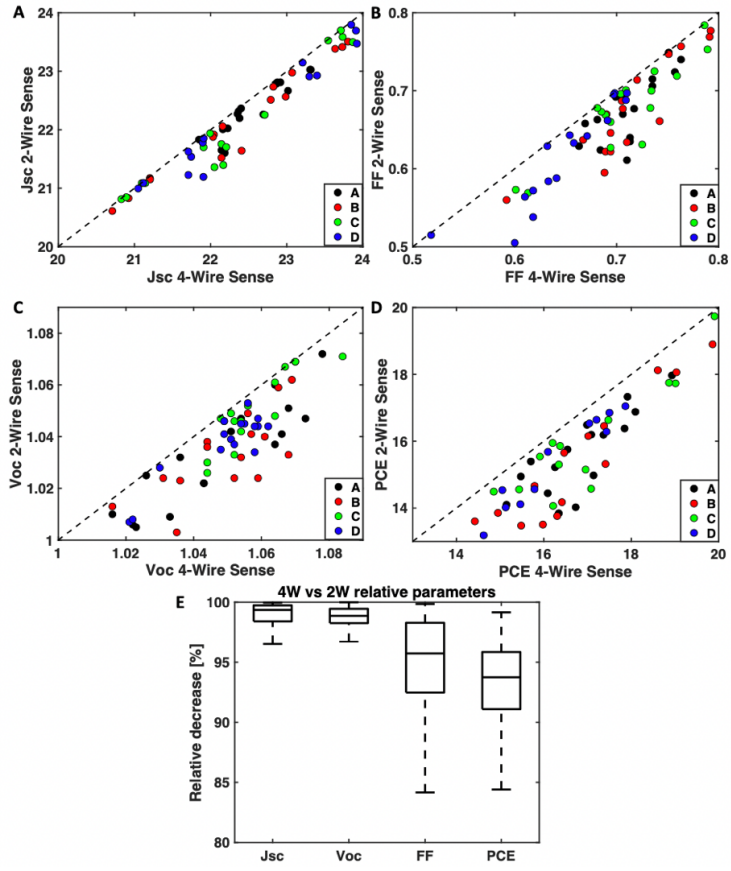

FIGURE 5 Comparison of metrics acquired using 2-wire and 4-wire sense technique. (A) J_{SC} (B) Fill Factor, (C) V_{OC} and (D) PCE of four different batches of 16 solar cells each (A, B, C, D). The diagonal line represents an equal measurement. (E) Provides relative summary of parameter decrease. A reduced standard deviation on the FF obtained by the automated measurement demonstrates the superior reliability of the measurements made with minimum human interaction. We attribute the reduced performance of the manual measurement to the sum of several minor errors, such as misalignments between the shadow mask and the electrode, and non-perpendicularity between the the sample and the incoming light. In addition, the lack of N_2 cooling and longer exposure to humidity and light, may contribute to slight degradation prior to the measurement.14-15, 17, 35

3 | CONCLUSIONS

In our work, we have developed a high-throughput solar simulator based system for perovskite solar cells for rapid combinatorial screening. This high-throughput solar cell characterization system is capable of performing measurements with high accuracy and allows for excellent versatility in terms of measurement protocols. The system provides rapid and reliable research-scale characterization for perovskite solar cells and other emerging solar cell technologies. Combined with the pre-patterned FTO substrate these automatic features can significantly increase the daily output of any research laboratory. We have shown the benefits of a 4-wire sense method for measuring perovskite solar cells, and its impact on the photovoltaic performance parameters. The system tackles commonly known issues found when measuring hysteretic PSCs and can potentially set a benchmark for PCS measurement protocols. We have demonstrated that by automating the solar simulator, we can potentially reduce the discovery time of novel perovskite materials. The high-throughput scanning improves the productivity of perovskite research laboratories, and removes human error by employing a systematic and repeatable method of characterization of PSCs.

Acknowledgements

The authors are grateful for the financial support by the Australian Research Council (ARC) ARC Centre of Excellence in Exciton Science (ACEx). The authors are grateful for the financial support by the Australian Research Council (ARC) discovery project (DP160104575), the Australian Centre for Advanced Photovoltaics (ACAP), the Australian Renewable Energy Agency, and the ARC Centre of Excellence in Exciton Science (ACEx:CE170100026). This work was performed in part at the Melbourne Centre for Nanofabrication (MCN) in the Victorian Node of the Australian National Fabrication Facility (ANFF).

Conflict of interest

No conflict of interest has been declared by the author(s).

Supplementary Information

The photocurrent response is measured during a voltage sweep from short circuit to open circuit (forward) and back to short circuit (reverse). The maximum power point (MPP) is the maximum power produced (P = V x I) and is used to determine the PCE. However, in contrast to conventional semiconductor based devices, hybrid perovskites and perovskite-like materials demonstrate a severe hysteresis, a strong variation of *J-V* curve between forward and reverse scan direction during *J-V* sweeps, which complicates determination of the true MPP and PCE.36

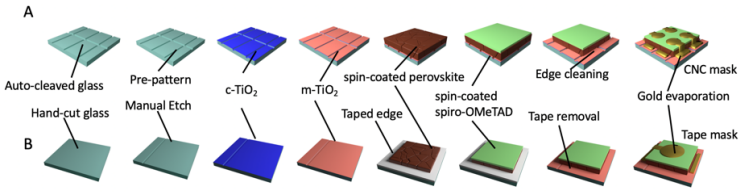

S1: Typical single cell substrate compared with our new multi-cell design fabrication steps. The new design process assures precise alignment and increases the number of cells per substrate, increasing the throughput of device fabrication by factor of about. (A) Old design requires researcher to manually cut, etch and mask to produce the device (B) Custom-fabricated precision-cut glass with machine pre-patterned etch lines, the substrate is placed inside the spray jig, after the spin coating the substrates are placed inside the evaporation jig.

To achieve that researcher has to remove conductive oxide somehow; the patterning is achieved using low power laser etching or chemical etching. Such substrates then get cleaned in staining jars and are immediately covered with electron transporting layer (ETL). Then next step is to mask areas that will be later used as contacting terminals with the tape and spin-coat the sample with perovskite precursor solution and hole transporting layer (HTL) with intermittent drying and annealing steps. Later on, the tape is removed in order to evaporate electrodes. The ultimate fabrication step is to deposit metal contacts, the substrate is masked using adhesive tape and the metal electrode layer is evaporated (see Fig.1A). A complete device is characterized using manually-aligned aperture mask to define the area exposed to sunlight. A very common procedure to measure the devices is to manually clip the two electrodes of the solar cell and illuminate the cell. However, the clips can damage the electrodes, typically a very thin (100 nm) layer of metal and/or make poor electrical contact. An alternative method is to solder wires to the electrodes which provide excellent contact. However, this process can heat the local area to temperatures in excess of 150 °C, which can induce damage or local structural/chemical changes in the device.37-39 It is obvious that such methods are very time-consuming for routine and systematic analysis and/or add undesired series resistances to the electrical measurements. Furthermore, by maintaining the exact distance between the light source and the measured cell, using a custom-designed solar simulator holder, aluminium extrusions for the x-y stage, along with a 3D printed chamber (Melbourne Centre for Nanofabrication, 16 µm feature precision), we assured perpendicularity between the incoming light and the substrates.

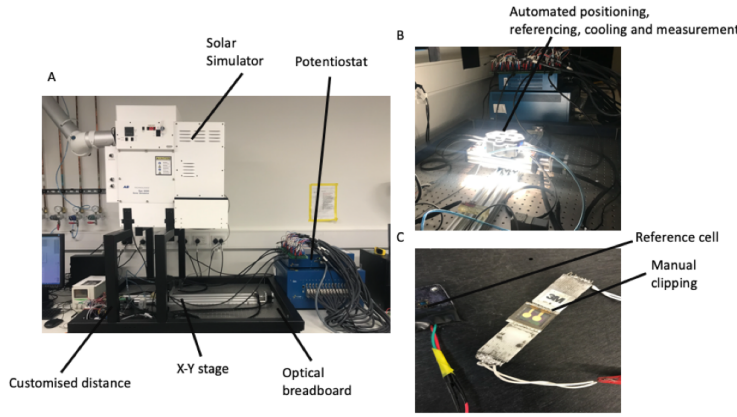

S2: The high-throughput solar cell characterization system. A) Picture of our system. B) Measurement in action using our automated method C) Picture of old style manual measurement approach.

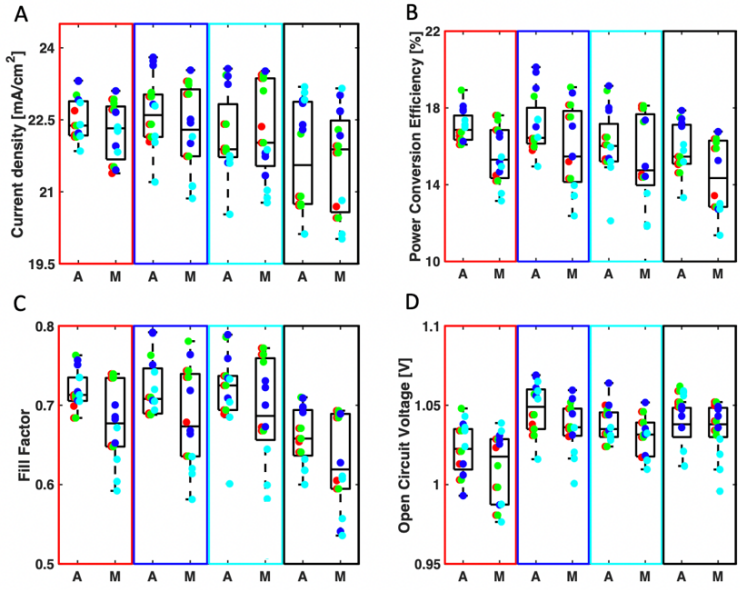

S3: The statistics of the photovoltaic parameters extracted from 4 batches of 16 cells measured using new automated technique and old manual. The automated measurement resulted in overall superior values for all parameters with reduced deviations; Champion cell: J_{SC} = 23.79 ± 0.01 mA/cm^2, V_{OC} = 1.07 ± 0.01 V, FF = 0.79 ± 0.01 and PCE = 20.12 ± 0.05 % compared to the manual mode; J_{SC} = 23.52 ± 0.01 mA/cm^2, V_{OC} = 1.06 ± 0.01 V, FF = 0.78 ± 0.01 and PCE = 19.75 ± 0.05 %.

The algorithm automatically processes the measurements and, by using the mask area input by the user, it provides an output file with the calculated photovoltaic parameters V_{OC}, J_{SC}, FF and PCE, using the equations commonly found in literature12, 14, 29, 40, readily used for further data analysis. The summary file has the batch code number, RAW

file with all measurements, graphical representation of immediate plots (less data points). The user has real-time option to observe formation of the plots (*J-V*, constant bias voltage stability and MPPT).

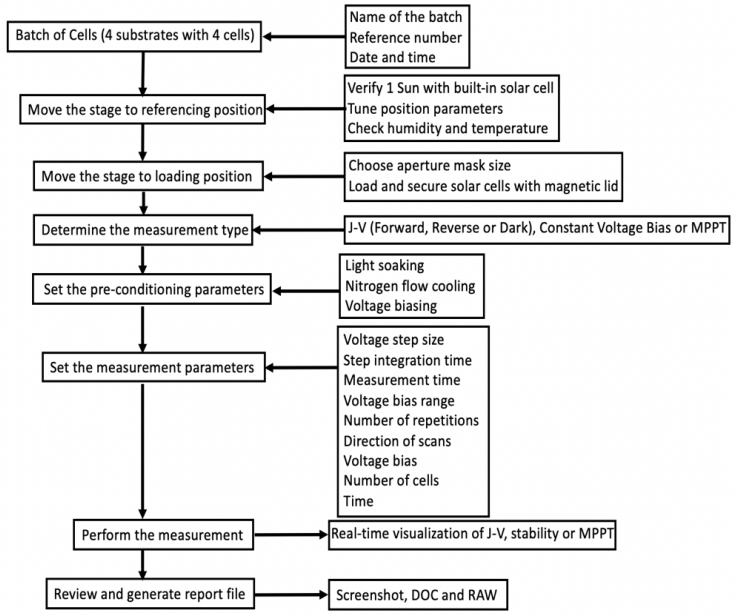

S4: Open-style protocol algorithm implemented in our software. It is designed to increase high-throughput and allow user to quickly adjust own parameters of the measurement whilst maintaining reproducing the same measurement conditions and track any changes that can occur during the measurement.

References

1. NREL Best Research-Cell Efficiency Chart. (https://www.nrel.gov/pv/cell-efficiency.html.

2. Eames, C.; Frost, J. M.; Barnes, P. R. F.; O'Regan, B. C.; Walsh, A.; Islam, M. S., Ionic transport in hybrid lead iodide perovskite solar cells. Nature Communications 2015, 6 (1), 7497.

3. Habisreutinger, S. N.; Noel, N. K.; Snaith, H. J., Hysteresis Index: A Figure without Merit for Quantifying Hysteresis in Perovskite Solar Cells. ACS Energy Letters 2018, 3 (10), 2472-2476.

4. Unger, E. L.; Hoke, E. T.; Bailie, C. D.; Nguyen, W. H.; Bowring, A. R.; Heumüller, T.; Christoforo, M. G.; McGehee, M. D., Hysteresis and transient behavior in current–voltage measurements of hybrid-perovskite absorber solar cells. Energy Environmental Science 2014, 7 (11), 3690-3698.

5. Snaith, H. J.; Abate, A.; Ball, J. M.; Eperon, G. E.; Leijtens, T.; Noel, N. K.; Stranks, S. D.; Wang, J. T.-W.; Wojciechowski, K.; Zhang, W., Anomalous Hysteresis in Perovskite Solar Cells. The Journal of Physical Chemistry Letters 2014, 5 (9), 1511-1515.

6. Pellet, N.; Giordano, F.; Ibrahim Dar, M.; Gregori, G.; Zakeeruddin, S. M.; Maier, J.; Grätzel, M., Hill climbing hysteresis of perovskite-based solar cells: a maximum power point tracking investigation. Progress in Photovoltaics: Research and Applications 2017, 25 (11), 942-950.

7. Chen, C.-Y.; Chang, J.-H.; Chiang, K.-M.; Lin, H.-L.; Hsiao, S.-Y.; Lin, H.-W., Perovskite Photovoltaics for Dim-Light Applications. Advanced Functional Materials 2015, 25 (45), 7064-7070.
8. Tress, W.; Domanski, K.; Carlsen, B.; Agarwalla, A.; Alharbi, E. A.; Graetzel, M.; Hagfeldt, A., Performance of perovskite solar cells under simulated temperature-illumination real-world operating conditions. Nature Energy 2019, 4 (7), 568-574.
9. Surface, S. T. f. R. S. S. I. D. N. a. H. o. T. ASTM G173 - 03(2008). http://www.astm.org/cgi-bin/resolver.cgi?G173.
10. Testing, S. S. f. S. S. f. T. P. ASTM E927 - 10. http://www.astm.org/cgi-bin/resolver.cgi?E927.
11. Zimmermann, E.; Ehrenreich, P.; Pfadler, T.; Dorman, J. A.; Weickert, J.; Schmidt-Mende, L., Erroneous efficiency reports harm organic solar cell research. Nature Photonics 2014, 8, 669.
12. Rakocevic, L.; Ernst, F.; Yimga, N. T.; Vashishtha, S.; Aernouts, T.; Heumueller, T.; Brabec, C. J.; Gehlhaar, R.; Poortmans, J., Reliable Performance Comparison of Perovskite Solar Cells Using Optimized Maximum Power Point Tracking. Solar RRL 2019, 3 (2), 1800287.
13. Moulé, A. J.; Meerholz, K., Morphology Control in Solution-Processed Bulk-Heterojunction Solar Cell Mixtures. Advanced Functional Materials 2009, 19 (19), 3028-3036.
14. Zimmermann, E.; Wong, K. K.; Müller, M.; Hu, H.; Ehrenreich, P.; Kohlstädt, M.; Würfel, U.; Mastroianni, S.; Mathiazhagan, G.; Hinsch, A.; Gujar, T. P.; Thelakkat, M.; Pfadler, T.; Schmidt-Mende, L., Characterization of perovskite solar cells: Towards a reliable measurement protocol. APL Materials 2016, 4 (9), 091901.
15. Dunbar, R. B.; Duck, B. C.; Moriarty, T.; Anderson, K. F.; Duffy, Noel W.; Fell, C. J.; Kim, J.; Ho-Baillie, A.; Vak, D.; Duong, T.; Wu, Y.; Weber, K.; Pascoe, A.; Cheng, Y.-B.; Lin, Q.; Burn, P. L.; Bhattacharjee, R.; Wang, H.; Wilson, G. J., How reliable are efficiency measurements of perovskite solar cells? The first inter-comparison, between two accredited and eight non-accredited laboratories. Journal of Materials Chemistry A 2017, 5 (43), 22542-22558.
16. Christians, J. A.; Manser, J. S.; Kamat, P. V., Best Practices in Perovskite Solar Cell Efficiency Measurements. Avoiding the Error of Making Bad Cells Look Good. The Journal of Physical Chemistry Letters 2015, 6 (5), 852-857.
17. Dunbar, R. B.; Moustafa, W.; Pascoe, A. R.; Jones, T. W.; Anderson, K. F.; Cheng, Y.-B.; Fell, C. J.; Wilson, G. J., Device pre-conditioning and steady-state temperature dependence of CH3NH3PbI3 perovskite solar cells. Progress in Photovoltaics: Research and Applications 2017, 25 (7), 533-544.
18. Mundhaas, N.; Yu, Z. J.; Bush, K. A.; Wang, H.-P.; Häusele, J.; Kavadiya, S.; McGehee, M. D.; Holman, Z. C., Series Resistance Measurements of Perovskite Solar Cells Using Jsc–Voc Measurements. Solar RRL 2019, 3 (4), 1800378.
19. O'Regan, B. C.; Barnes, P. R. F.; Li, X.; Law, C.; Palomares, E.; Marin-Beloqui, J. M., Optoelectronic Studies of Methylammonium Lead Iodide Perovskite Solar Cells with Mesoporous TiO2: Separation of Electronic and Chemical Charge Storage, Understanding Two Recombination Lifetimes, and the Evolution of Band Offsets during J–V Hysteresis. Journal of the American Chemical Society 2015, 137 (15), 5087-5099.
20. Measurements, P. Multichannel Solar Characterization Systems. http://www.pvmeasurements.com/Products/I-V-Measurements/solar-cell-i-v-data-acquisition-system.html.
21. Pellet, C. S. N. Multichannel Solar Characterization Setup. contact@candlelight-systems.com.
22. Ossila Solar characterization System. https://www.ossila.com/products/solar-cell-iv-test-system?variant=13633049100384.
23. Instruments, N. 1-channel SMU. http://www.ni.com/en-au/support/model.pxi-4130.html http://www.ni.com/example/30918
24. Snaith, H. J., How should you measure your excitonic solar cells? Energy Environmental Science 2012, 5 (4), 6513-6520.
25. Ito, S.; Nazeeruddin, M. K.; Liska, P.; Comte, P.; Charvet, R.; Péchy, P.; Jirousek, M.; Kay, A.; Zakeeruddin, S. M.; Grätzel, M., Photovoltaic characterization of dye-sensitized solar cells: effect of device masking on conversion efficiency. Progress in Photovoltaics: Research and Applications 2006, 14 (7), 589-601.
26. Kiermasch, D.; Gil-Escrig, L.; Bolink, H. J.; Tvingstedt, K., Effects of Masking on Open-Circuit Voltage and Fill

Factor in Solar Cells. Joule 2019, 3 (1), 16-26.
27. Chen, Q.; Chen, L.; Ye, F.; Zhao, T.; Tang, F.; Rajagopal, A.; Jiang, Z.; Jiang, S.; Jen, A. K. Y.; Xie, Y.; Cai, J.; Chen, L., Ag-Incorporated Organic–Inorganic Perovskite Films and Planar Heterojunction Solar Cells. Nano Letters 2017, 17 (5), 3231-3237.
28. International, A., ASTM E927-10. West Conshohocken, PA, 2010.
29. Shrotriya, V.; Li, G.; Yao, Y.; Moriarty, T.; Emery, K.; Yang, Y., Accurate Measurement and Characterization of Organic Solar Cells. Advanced Functional Materials 2006, 16 (15), 2016-2023.
30. Wang, Y.; Liu, X.; Zhou, Z.; Ru, P.; Chen, H.; Yang, X.; Han, L., Reliable Measurement of Perovskite Solar Cells. Advanced Materials 2019, 0 (0), 1803231.
31. Zhao, C.; Chen, B.; Qiao, X.; Luan, L.; Lu, K.; Hu, B., Revealing Underlying Processes Involved in Light Soaking Effects and Hysteresis Phenomena in Perovskite Solar Cells. Advanced Energy Materials 2015, 5 (14), 1500279.
32. Xu, X.; Shi, J.; Wu, H.; Yang, Y.; Xiao, J.; Luo, Y.; Li, D.; Meng, Q., The influence of different mask aperture on the open-circuit voltage measurement of perovskite solar cells. Journal of Renewable and Sustainable Energy 2015, 7 (4), 043104.
33. Saliba, M.; Correa-Baena, J.-P.; Wolff, C. M.; Stolterfoht, M.; Phung, N.; Albrecht, S.; Neher, D.; Abate, A., How to Make over 20% Efficient Perovskite Solar Cells in Regular (n–i–p) and Inverted (p–i–n) Architectures. Chemistry of Materials 2018, 30 (13), 4193-4201.
34. Fu, F.; Feurer, T.; Weiss, Thomas P.; Pisoni, S.; Avancini, E.; Andres, C.; Buecheler, S.; Tiwari, Ayodhya N., High-efficiency inverted semi-transparent planar perovskite solar cells in substrate configuration. Nature Energy 2016, 2, 16190.
35. Jena, A. K.; Kulkarni, A.; Miyasaka, T., Halide Perovskite Photovoltaics: Background, Status, and Future Prospects. Chemical Reviews 2019, 119 (5), 3036-3103.
36. Chen, B.; Yang, M.; Priya, S.; Zhu, K., Origin of J–V Hysteresis in Perovskite Solar Cells. The Journal of Physical Chemistry Letters 2016, 7 (5), 905-917.
37. Ke, J. H.; Yang, T. L.; Lai, Y. S.; Kao, C. R., Analysis and experimental verification of the competing degradation mechanisms for solder joints under electron current stressing. Acta Materialia 2011, 59 (6), 2462-2468.
38. Han, Y.; Meyer, S.; Dkhissi, Y.; Weber, K.; Pringle, J. M.; Bach, U.; Spiccia, L.; Cheng, Y.-B., Degradation observations of encapsulated planar CH3NH3PbI3 perovskite solar cells at high temperatures and humidity. Journal of Materials Chemistry A 2015, 3 (15), 8139-8147.
39. Lanin, V. L., Ultrasonic soldering in electronics. Ultrasonics Sonochemistry 2001, 8 (4), 379-385.
40. Schwander, D. In Dynamic Solar Cell Measurement Techniques: New Small Signal Measurement Techniques, Space Power, May 01, 2002; 2002; p 603.